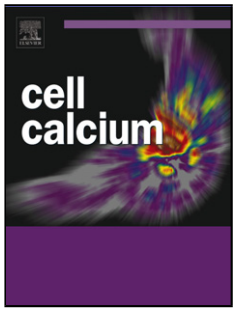

Title: Evidence for the interaction of peroxiredoxin-4 with the store-operated calcium channel activator STIM1 in liver cells

Authors: Ka Cheung Tam, Eunus Ali, Jin Hua, Tim Chataway, Greg J. Barritt

PII: S0143-4160(18)30028-9
DOI: https://doi.org/10.1016/j.ceca.2018.05.002
Reference: YCECA 1942

To appear in: *Cell Calcium*

Received date: 11-2-2018
Revised date: 4-5-2018
Accepted date: 12-5-2018

Please cite this article as: Tam KC, Ali E, Hua J, Chataway T, Barritt GJ, Evidence for the interaction of peroxiredoxin-4 with the store-operated calcium channel activator STIM1 in liver cells, *Cell Calcium* (2010), https://doi.org/10.1016/j.ceca.2018.05.002

Evidence for the interaction of peroxiredoxin-4 with the store-operated calcium channel activator STIM1 in liver cells

Ka Cheung Tam, Eunus Ali, Jin Hua, Tim Chataway and Greg J. Barritt

Discipline of Medical Biochemistry, College of Medicine and Public Health, Flinders University, Adelaide, South Australia, 5001, Australia

To whom correspondence and reprint requests should be addressed:

Professor Greg J. Barritt

Discipline of Medical Biochemistry

College of Medicine and Public Health,

Flinders University

GPO Box 2100

Adelaide SA 5001

Australia

Tel: +61 438 204 426

Email: greg.barritt@flinders.edu.au

Graphical abstarct

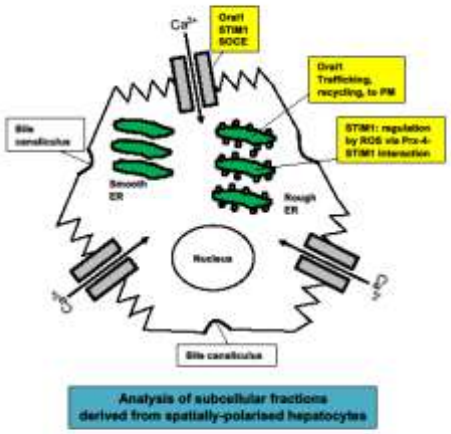

Highlights

- Orai1 is predominantly located in the heavy and light microsomes in rat liver
- STIM1 is predominantly located in the heavy and light microsomes in rat liver
- STIM1 interacts with peroxiredoxin-4 in heavy microsomes derived from liver
- Peroxiredoxin-4 alters the susceptibility of STIM1 to inhibition by H_2O_2

ABSTRACT

Ca^{2+} entry through store-operated Ca^{2+} channels (SOCs) in the plasma membrane (PM) of hepatocytes plays a central role in the hormonal regulation of liver metabolism. SOCs are composed of Orai1, the channel pore protein, and STIM1, the activator protein, and are regulated by hormones and reactive oxygen species (ROS). In addition to Orai1, STIM1 also interacts with several other intracellular proteins. Most previous studies of the cellular functions of Orai1 and STIM1 have employed immortalised cells in culture expressing ectopic proteins tagged with a fluorescent polypeptide such as GFP. Little is known about the intracellular distributions of endogenous Orai1 and STIM1. The aims are to determine the

intracellular distribution of endogenous Orai1 and STIM1 in hepatocytes and to identify novel STIM1 binding proteins. Subcellular fractions of rat liver were prepared by homogenisation and differential centrifugation. Orai1 and STIM1 were identified and quantified by western blot. Orai1 was found in the PM (0.03%), heavy (44%) and light (27%) microsomal fractions, and STIM1 in the PM (0.09%), and heavy (85%) and light (13%) microsomal fractions. Immunoprecipitation of STIM1 followed by LC/MS or western blot identified peroxiredoxin-4 (Prx-4) as a potential STIM1 binding protein. Prx-4 was found principally in the heavy microsomal fraction. Knockdown of Prx-4 using siRNA, or inhibition of Prx-4 using conoidin A, did not affect Ca^{2+} entry through SOCs but rendered SOCs susceptible to inhibition by H_2O_2. It is concluded that, in hepatocytes, a considerable proportion of endogenous Orai1 and STIM1 is located in the rough ER. In the rough ER, STIM1 interacts with Prx-4, and this interaction may contribute to the regulation by ROS of STIM1 and SOCs.

Abbreviations: $[Ca^{2+}]_{cyt}$, cytoplasmic free Ca^{2+} concentration; $Ca^{2+}{}_{ext}$, extracellular Ca^{2+}; ER, endoplasmic reticulum; PM, plasma membrane; SERCA, sarco/endoplasmic reticulum (Ca^{2+} +Mg^{2+})ATP-ase; PMCA, plasma membrane (Ca^{2+} +Mg^{2+})ATP-ase; SOCE, store-operated Ca^{2+} entry; SPCA, secretory pathway Ca^{2+} ATP-ase; SOC, store-operated Ca^{2+} channel; STIM, stromal interaction molecule; $[Ca^{2+}]_{ext}$, extracellular free Ca^{2+} concentration; DBHQ, 2,5-di-(*tert*-butyl)-1,4-benzohydro-quinone; GFP, green fluorescent protein; Prx-4, peroxiredoxin-4; TRPM2, transient receptor potential melastatin 2; PMSF, phenylmethylsulfonyl fluoride; ROS, reactive oxygen species; HRP, horse radish peroxidase.

Key words: Store-operated Ca^{2+} channels; STIM1; Orai1; liver; subcellular fractionation; peroxiredoxin-4.

1. Introduction

Store-operated Ca^{2+} channels (SOCs) in the plasma membrane (PM), and Ca^{2+} entry through these channels (SOCE), play essential roles in the regulation by intracellular Ca^{2+} of cell growth, death and function in almost all animal cell types [1]. SOCE replenishes the ER Ca^{2+} stores during and after $InsP_3$-mediated Ca^{2+} release induced by hormones and other extracellular signals. In some situations SOCE contributes directly to changes in the cytoplasmic free Ca^{2+} concentration ($[Ca^{2+}]_{cyt}$) induced by extracellular signals [1, 2]. In addition to hormonal signals, reactive oxygen species (ROS) can also alter SOCE in both normal and pathological conditions (reviewed in [3, 4]). Most SOCs are composed of Orai1 polypeptides, which constitute the channel pore located in the PM, and STIM1 polypeptides located in the endoplasmic reticulum (ER), which activate Orai1 (reviewed in [1]).

SOC activation is initiated by a decrease in the Ca^{2+} concentration in the lumen of a sub-region of the ER which is devoid of ribosomes and located in ER-PM junctions at the periphery of the cell [1, 5, 6]. This leads to the dissociation of Ca^{2+} from the luminal E, F hand-sterile alpha (EF-SAM) Ca^{2+} binding motif in the N-terminal of STIM1, conformational changes in STIM1, movement of STIM1 in the plane of the ER membrane, interaction of the cytoplasmic CRAC activation domain (CAD) in the C-terminal of STIM1 with Orai1 located in the PM, and formation of an active functional SOC [1, 7]. Functional SOCs are composed of a hexamer of Orai1 polypeptides and approximately 4 STIM1 polypeptides [1, 7]. It is generally thought that in order to achieve SOCE activation, Orai1 must be present in the PM and STIM1 in the peripheral ER, located in close proximity to the plasma membrane [1]. The results of other studies have provided evidence for the interaction of STIM1 with

numerous other intracellular proteins (reviewed in [8]). Some of these STIM1-binding proteins modulate the interaction of STIM1 with Orai1 or modulate other proteins involved in intracellular Ca^{2+} homeostasis, while others are involved in regulation of the microtubular network [8-10].

Most previous studies on the intracellular distribution of Orai1 and STIM1 have been conducted using immortalised cells in culture over-expressing ectopic Orai1 and STIM1 tagged with a fluorescence peptide such as GFP, or variants of GFP [1, 11-16]. Much less is known about the distribution of endogenous Orai1 and STIM1 *in situ*. We have previously characterised SOCs in hepatocytes. These cells express functional SOCs with high selectivity for Ca^{2+}, and channel properties essentially identical to those in lymphocytes and mast cells [17]. While each of the main isoforms of STIM and Orai has been detected in rat hepatocytes and in immortalised H4IIE rat liver cells, the expression of STIM2 is lower than that of STIM1, Orai2 is barely detectable, and expression of Orai3 is much lower than that of Orai1 [18]. Previous studies, in which expression of STIM1 and Orai1 has been knocked down by siRNA, indicate that SOCs in rat hepatocytes and in H4IIE rat liver cells are principally composed of the STIM1 and Orai1 polypeptides [17, 19]. Our previous studies employing GFP- or Cherry-STIM1 have shown that, upon the release of Ca^{2+} from the ER, STIM1 forms puncta and moves to the PM [20, 21].

The aims of this study were to investigate the intracellular distribution of endogenous Orai1 and STIM1 in hepatocytes and to seek to identify additional novel proteins which may modify the action of STIM1. The experiments have employed the preparation and analysis of subcellular fractions of rat liver. The bulk of the liver is composed of hepatocytes which are the principle cell type responsible for liver-specific functions [22]. Moreover, liver tissue provides a good starting point for subcellular fractionation since it is easily homogenised, and

high yields of each subcellular fraction can be obtained [23]. A subcellular fractionation approach, rather than an alternative one based on immunofluorescence and confocal imaging, was chosen since we and others have found that it is sometimes difficult to obtain antibodies against PM ion channel proteins such as Orai1 and members of the TRP family with sufficient specificity [24, 25]. Furthermore, we wanted to employ immunoprecipitation and LC/MS to identify new STIM1 binding partners. This strategy requires relatively large amounts of protein, which can be obtained by liver homogenisation and subcellular fractionation.

2. Materials and methods

2.1. Materials

Phenylephrine was purchased from Sigma, St. Louis, MO USA; Conoidin A from the Cayman Chemical Company, whole serum (# R-1593-100) from Biosensis, Thebarton, South Australia; Protein A/G PLUS-Agarose immunoprecipitation reagent (#SC2003), normal mouse IgG (#SC-2025) and normal rabbit IgG (# sc-2027) from Santa Cruz Biotechnology, Dallas, Texas, USA, and protein ladders (markers) for western blot from BioRad Laboratories, New South Wales, Australia. The sources of the primary and secondary antibodies are listed in Table 1. The sources of all other materials were as described previously [18, 26, 27].

2.2. Rat liver homogenisation

Male Hooded Wistar rats weighing 250-350g, housed in the Flinders Medical Centre Animal Facility, were provided *ad libitum* access to food and water, with a lighting cycle of 12 h. Animals received humane care, and the experimental protocols were conducted according to the criteria outlined in the "Australian Code of Practice for the Care and Use of Animals for Scientific Purposes" (National Health and Medical Research Council of Australia). Removal of the liver and homogenisation of the liver were performed as described

by Lievrement et al. [28]. Rats were sedated with isoflurane then anesthetized by an intraperitoneal injection of ketamine (100 mg/kg body weight) and xylazine (8 mg/kg body weight). The homogenisation medium was composed of 250 mM sucrose, 5 mM HEPES-KOH and 1 mM EGTA, adjusted to pH 7.4, and supplemented with 1 mM dithiothreitol, and the proteolytic inhibitors 0.2 mM phenylmethylsulfonyl fluoride (PMSF), 10 µg/ml leupeptin, 10 µM pepstatin A, 2 µM benzamide, 5 µg/ml aprotinin, 50 µg/ml trypsin inhibitor, and 1 µg/ml *O*-phenanthroline. Homogenisation was performed using 10 passes of the loose-fitting pestle, and 3 passes of the tight-fitting pestle, of a 40 ml Dounce homogeniser (Kontes, DWK Life Sciences (Kimble)).

2.3. Preparation of subcellular fractions

The preparation of subcellular fractions was based on procedures previously developed by Lievrement et al. and Prpic et al. [28, 29]. The liver homogenate was centrifuged at 1,500 g for 10 min. This yielded a low speed pellet, which contains microsomes derived from the nuclear membrane and the PM, and a supernatant, which contains mitochondria, microsomes derived from the rough and smooth ER, other organelles, and cytosolic proteins [23, 28]. The pellet was resuspended in 2 ml of 250 mM sucrose, 25 mM HEPES-KOH, adjusted to pH to7.4, containing the proteolytic inhibitors listed above (Wash Medium) to give a final volume of about 12 ml. Two different subcellular fractionation strategies, designated the "Microsomal and Plasma Membrane Fractionation" strategy and the "Mitochondria, Microsomal and Cytosolic Fractionation" strategy, were then employed. In the first (the Microsomal and Plasma Membrane Fractionation), the re-suspended low speed pellet was used to prepare a PM fraction using Percoll gradient centrifugation as described by Prpić et al. [29]. The PM fraction was finally suspended in about 1 ml of 250 mM sucrose, 50 mM Tris-HCl, pH 8. To prepare the heavy and light microsomal fractions, the low speed

supernatant was centrifuged at 8,000 g for 20 min. The resulting pellet (the mitochondrial fraction) was discarded. The supernatant was centrifuged at 35,000 g for 30 min to yield a pellet of heavy microsomes and a supernatant containing light microsomes. The 35,000 g supernatant was then centrifuged at 100,000 g for 60 min to yield a pellet of light microsomes and a cytosolic fraction which was discarded. The heavy and light microsomal pellets were each resuspended by adding 6 ml Wash Medium. In the second subcellular fractionation strategy (the Mitochondria, Microsomal and Cytosolic Fractionation), the low speed pellet was retained for analysis (designated "low speed pellet") while the low speed supernatant was used to prepare a mitochondrial fraction, heavy and light microsomal fractions, and a cytosolic fraction. The low speed (1,500 g) supernatant was centrifuged at 8,000 g for 20 min. The resulting pellet (the mitochondrial fraction) was resuspended in 6 ml of Wash Medium. The supernatant was centrifuged at 35,000 g for 30 min to yield a pellet of heavy microsomes and a supernatant, containing light microsomes. The 35,000 g supernatant was then centrifuged at 100,000 g for 60 min to yield a pellet of light microsomes and the cytosolic fraction. The heavy and light microsomal pellets were each resuspended by adding 6 ml Wash Medium. The concentration of protein in the liver homogenate and in each subcellular fraction was determined by the EZQ method [30], as described previously [18, 27].

2.4 Treatment of livers with phenylephrine

Rats were anesthetized as described above and laparotomy performed to expose the inferior vena cava and the liver. Phenylephrine (1 mM stock solution in 0.9% (w/v) NaCl) was injected into the inferior vena cava to give an estimated initial blood concentration of 15 μM phenylephrine, based on a blood volume of 7.5 ml per 100 g body weight [31]. After 20 min, a blood sample (500 μl) was taken from the inferior vena cava, and the liver removed

and homogenised as described above. During the administration of phenylephrine, the breathing and heart rate and degree of secretion from the mouth were monitored in order to confirm that phenylephrine induced the expected physiological responses [32]. Blood glucose concentrations were measured spectrophotometrically by the glucose oxidase method, using an assay kit Sigma (GAGO-20), according to the manufacturer's instructions.

2.5. Culture of H4IIE rat liver cells and transfection with siRNA for knockdown of peroxiredoxin-4

The source of H4IIE rat liver cells and conditions of cell culture were as described previously [18, 20, 33]. H4IIE cells attached to coverslips were co-transfected with Silencer ® Select Pre-Designed siRNA (Life Technologies™) targeting rat peroxiredoxin-4 (Catalog #: 4390771, Serial: s136933 and s136935) using Lipofectamine® RNAiMAX transfection reagent (Life Technologies™), according to the manufacturer's instructions. As a negative control, cells were transfected with Silencer® Select Negative Control (Catalogue #: 439084, (Life Technologies™).

2.6. Western blots

Western bots were performed as described previously [18, 27]. Samples of subcellular fractions were mixed with 50 mM Tris-HCl, pH 6.6, containing 2% (w/v) SDS, 0.1% (w/v) bromophenol blue, 10% (v/v) glycerol and 100 mM dithiothreitol (Sample Loading Buffer), and heated at 87°C for 10 min. PVDF membranes were blocked with skim milk (5% w/v) dissolved in Tris buffer solution containing Tween20 (0.1%) (Blocking Buffer) for 1h at room temperature. Secondary antibodies conjugated with horse radish peroxidase (HRP) were used to visualise protein bands on the PVDF membrane. All secondary antibodies were diluted in Blocking Buffer. Protein bands were visualised using enhanced chemiluminescence detection reagent (SuperSignal® Western Pico substrate, Thermo Scientific) and a FujiFilm LAS4000

Imager. Image resolution was set to a standard setting of 1536 x1024 pixels and the time of exposure was 10 min. The same resolution and exposure time were used in all experiments in order to allow quantitative comparison of the results. Band intensity was quantified using MultiGauge software (FujiFilm). Local background was subtracted, and the resulting value was normalised by the amount of protein loaded onto the gel.

The origins and dilutions of the primary and secondary antibodies employed, the bands detected, and references for the expected size of each band are listed in Table 1. In order to quantitate the amount of a given protein in each subcellular fraction, and to compare the relative amount of a given protein between different subcellular fractions, the region over which band intensity was a linear function of the amount of protein applied to the gel was determined for calreticulin, PMCA, STIM1 and Orai1 (Fig. 1 and Supplemental Data Fig. S1). To determine the relative amounts of calreticulin, PMCA, STIM1 and Orai1 in each sub-cellular fraction, western blots of the protein present in a given subcellular fraction were conducted. The amount of protein applied to the gel (normally 10 to 30 ug per lane) was chosen so as to be in the middle of the linear range shown in Fig. 1. The intensity of the protein band was determined (working within the linear range shown in Fig. 1) and was expressed as intensity units per mg protein or as intensity units per total volume of subcellular fraction.

2.7. Immunoprecipitation of STIM1 from the heavy microsomal fraction

The method employed for immunoprecipitation was based on that described previously [26]. Heavy microsomes were dissolved in 150 mM NaCl containing 50 mM Tris-HCl , 5 mM EGTA, 1% (v/v) Nonidet P-40, 0.25% (w/v) sodium deoxycholate , 0.1% (w/v) sodium dodecyl sulphate supplemented with the proteolytic inhibitors 0.2 mM PMSF, 10 µM pepstatin A, 10 µg/ml leupeptin (Lysis Buffer) to give a final protein concentration of 5 mg/ml. Samples of this protein extract were incubated at 4°C overnight with 1 µg anti-STIM1 antibody (Abcam, # 52458). Protein A/G PLUS-Agarose (20µl) was then added, and

the mixture incubated at 4°C for another 4 h. The immunoprecipitated proteins and Protein A/G PLUS-Agarose were collected by centrifugation at 15,000 g for 10 min at 4°C, and washed 3 times with Lysis Buffer. Sample Loading Buffer (40 µl) was added to the immunoprecipitate, which included Protein A/G PLUS-Agarose, and the mixture heated at 87°C for 10 min to elute proteins bound to the Protein A/G PLUS-Agarose. The eluted proteins were separated from Protein A/G PLUS-Agarose by centrifugation at 15,000 g for 1 min, and were analysed by western blot, as described above, using Any kD™ Mini-PROTEAN® TGX™ Precast Protein Gels (Bio-Rad Laboratories). STIM1 and Prx-4 bands on the PDF membrane were detected using anti-STIM1 antibody (Abcam, # 52458) or anti-Prx-4 antibody (Biosensis, # R-1593-100), respectively.

2.8. Identification of proteins in STIM1 immunoprecipitates by LC/MS

Proteins present in STIM1 immunoprecipitates, prepared as described above, were identified by LC/MS, as described previously [27]. The resulting spectra were analysed using the SEQUEST algorithm (Version 1.2) against the rat International Protein Index (IPI) database (Version 3.74, 39,708 protein entries).

2.8. Measurement of intracellular Ca^{2+} and store-operated Ca^{2+} entry

$[Ca^{2+}]_{cyt}$ was measured in cells attached to glass coverslips at 37°C using Fura-2 and fluorescence imaging microscopy, with an image acquisition time of one image every 10 sec, as described previously [18, 21, 34]. The fluorescence ratio (F_{340nm}/F_{380nm}) was converted to changes in $[Ca^{2+}]_{cyt}$ according to Grynkiewicz, Poenie and Tsien [35]. Amounts of Ca^{2+} released were determined by measuring the height of the peak of the DBHQ-induced increase in $[Ca^{2+}]_{cyt}$. Initial rates of Ca^{2+} entry were measured using a "Ca^{2+} add-back" protocol, as described previously [18, 21].

2.9. Statistics

Unless stated otherwise, results are expressed as means ± SEM. Statistical significance (P<0.05) was determined between groups using one-way analysis of variance (ANOVA) followed by Newman-Keuls multiple comparison *post hoc* test or Student's t-test (two tailed, unpaired).

3. Results

3.1. STIM1 and Orai1 are enriched in the microsomal fractions of rat liver

To determine the distribution of STIM1 and Orai1 in subcellular fractions of rat liver, untreated livers and livers pre-treated with phenylephrine and were homogenised, and the homogenate initially subjected to centrifugation at 1,500 g for 10 min. This yielded a low speed pellet, which contains microsomes derived from the nuclear membrane and the PM and a supernatant, which contains mitochondria, microsomes derived from the rough and smooth ER, other organelles and cytosolic proteins [23, 28]. Two different subcellular fractionation strategies were then employed. In first (the Microsomal and Plasma Membrane Fractionation), the low speed pellet was used to prepare a PM fraction using Percoll gradient centrifugation. Heavy and light microsomal fractions were prepared from the low speed supernatant. In the second (the Mitochondria, Microsomal and Cytosolic Fractionation), the low speed pellet was retained for analysis while the low speed supernatant was used to prepare a mitochondrial fraction, heavy and light microsomal fractions, and a cytosolic fraction.

The distribution of the ER marker protein calreticulin [36] and the PM marker protein PMCA [37-39] in subcellular fractions derived from untreated livers was determined by western blot and subsequent quantitation of the amounts of protein in the bands

corresponding to calreticulin and PMCA. The results are shown in Fig. 2 and in Supplemental Data Fig.S2). Relative to whole liver, calreticulin was enriched in the heavy microsomes, light microsomes, and mitochondria (Fig. 2A-C). The detection of some calreticulin in the PM subcellular fraction may be due, in part, to: the presence, in the PM subcellular fraction, of some microsomes derived from the ER, and/or to the localisation of some calreticulin in the PM itself in intact hepatocytes [40]. PMCA was principally enriched in the in the PM fraction (Fig. 2 A, D). These results provide evidence that the fractions designated "heavy microsomes" and "light microsomes" are enriched in microsomes derived from the ER, and that the fraction designated "PM" is enriched in microsomes derived from the PM.

The distribution of STIM1 and Orai1 in subcellular fractions derived from untreated livers is shown in Figs. 3 and 4 (expressed as relative units of band intensity per mg protein), in Table 2 (expressed as relative units of band intensity per total volume of fraction), and in Supplemental Data Figs. S3 and S4. The sizes of the bands detected by the anti-1 STIM1 and anti-Orai1 antibodies were 75 and 45 kDa, respectively (Figs. 3 and 4 and Supplemental Data Figs. 3 and 4). The size (45 kDa) of the band detected by the anti-Orai1 antibody corresponds to the glycosylated form of Orai1[16, 41] and is similar to the size of endogenous Orai1 observed previously in hepatocytes and liver cells [18] and in other mammalian cell types [42, 43]. Relative to whole liver, STIM1 was enriched in the heavy and light microsomal fractions, with no detectable enrichment in the PM fraction or in the low speed pellet (Fig. 3). Others have previously shown that the low speed pellet contains microsomes derived from the PM [29]. About 85% of all the STIM1 was found in the heavy microsomal fraction (Table 2). Orai1 was enriched in the heavy and light microsomal fractions with little enrichment in the PM fraction (Fig. 4). About 50% of all the Orai1 was found in the heavy microsomal fraction (Table 2).

On the basis of many previous studies [1, 11, 16], it had been expected that Orai1 would be principally located in the PM fraction, rather than in microsomal fractions derived from the ER. In view of this somewhat unexpected observation, we compared the distribution of Orai1 with that of another ion channel protein, the transient receptor potential melastatin 2 (TRPM2) non-selective cation channel, thought to be principally located in the PM of animal cells [34]. TRPM2 is expressed in rat hepatocytes and is functional in the PM [34]. Relative to whole liver, TRPM2 was enriched in the low speed pellet (which contains PM vesicles) and mitochondria (Fig. 5 A,B). In contrast to Orai1, no enrichment of TRPM2 was observed in the heavy or light microsomal fractions.

In some cell types, it has been shown that, in addition to its role in forming SOCs in the PM, Orai1 is located in acidic intracellular stores, including secretory granules, where it mediates Ca^{2+} release from these granules [44, 45]. Therefore, we also compared the distribution of Orai1 in liver subcellular fractions with that of two secretory granule marker proteins, secretory pathway Ca^{2+} ATP-ase 1 and 2 (SPCA1 and SPCA2), using an antibody which recognises both of these proteins. While SPCA1 and SPCA2 were difficult to detect in western blots, SPCA1 was enriched principally in the cytosolic and light microsomal fractions, while SPCA2 was principally enriched in the cytosolic fraction with little enrichment in the light or heavy microsomal fractions (Fig. 5C). Comparison of the distribution in subcellular fractions of SPCA1 and 2 with that of Orai1 suggests that the location of Orai1 in secretory granules is unlikely to account for the large amount of Orai1 found in the heavy microsomal fraction.

3.2. Pre-treatment with phenylephrine does not lead to a detectable change in the distribution of STIM1 or Orai1 in sub-cellular fractions of rat liver

The results of many experiments employing cells transfected with STIM1 tagged with a fluorescent polypeptide such as GFP, have shown that Ca^{2+} release from the ER causes STIM1 to form puncta and increases the amount of STIM1 associated with the PM [1]. To determine whether the release of Ca^{2+} from the ER and the subsequent activation of SOCE lead to a detectable change in the distribution of STIM1 and/or Orai1 in liver subcellular fractions, livers were pre-treated *in vivo* with phenylephrine, an α-adrenergic agonist which activates SOCE in hepatocytes [46]. As shown previously [47], following 20 min exposure to phenylephrine, the blood glucose concentration was increased to 28 ± 2 mM compared with controls 19 ± 2 mM (means ± SEM, n=3). (The blood glucose concentration in both control and phenylephrine-treated rats was elevated by the ketamine xylazine anaesthesia [48]). Phenylephrine pre-treatment did not cause a detectable change in the distribution of STIM1 or Orai1 (Figs. 3 and 4, and Table 2).

3.3. Identification of peroxiredoxin-4 as a potential STIM1 binding protein

The results described above have shown that, in subcellular fractions of liver, STIM1 is predominantly located in the heavy microsomal fraction (derived from the rough ER) with some in the light microsomal fraction (derived from the smooth ER). The activation of Orai1 by STIM1 occurs in the cortical ER [5, 6]. This is devoid of ribosomes and hence, upon homogenisation of the whole liver, is likely to generate microsomes which sediment in the light microsomal fraction. On the one hand, STIM1 located in heavy microsomes is unlikely to be directly involved in the activation of Orai1. On the other hand, it has been shown that STIM1 can interact with a number of other proteins as well as with Orai1. Many of these are located in the rough ER [8]. Therefore, we searched for STIM1 binding proteins in the heavy microsomal fraction. The strategy employed was to immunoprecipitate STIM1 using an anti-STIM1 antibody, then analyse proteins in the immunuprecipitae using LC/MS.

To confirm that STIM1 could be immunoprecipitated from proteins extracted from the heavy microsomal fraction, western blot was used to determine whether STIM1 was present in the immunoprecipitate obtained using an anti-STIM1 antibody. The results indicate that STIM1 is enriched in the immunoprecipitate (Fig. 6A). Proteins present in immunoprecipitates obtained using the anti-STIM1 antibody were hydrolysed and the peptides analysed by LC/MS. Table 3 lists fourteen proteins which were identified in the ant-STIM1 immunoprecipitate but were not present in the IgG control. These proteins include STIM1, keratin, nuclear binding proteins, peroxiredoxin-4 (Prx-4), as well as several other proteins. The presence of STIM1 confirms that the immunoprecipitation was successful. Keratin and ProteinKrt16 are likely to be skin contaminants [49] and some nuclear binding proteins are known to bind non-specifically to agarose beads employed for the immunoprecipitation [50]. Prx-4 was of interest since several studies have shown that SOCE, and STIM1 and Orai1, can be modified by ROS [3, 4]. Moreover, it is known that Prx-4 is located in the lumen of the ER where, together with a protein disulphide isomerase and ER oxidoreductase 1, it is thought to catalyse the conversion of H_2O_2 to H_2O [51-54].

The potential interaction of Prx-4 with STIM1 was investigated further by determining the distribution of Prx-4 in subcellular fractions of liver using western blot. Two bands of Prx-4 were detected, corresponding to the Prx-4 monomer (25 kDa) and dimer (50 kDa) [53, 55] (Fig. 6B). Prx-4 was principally enriched in the heavy microsomal fraction with some enrichment in the light microsomal and mitochondrial fractions (Fig. 6B,C). Immunoprecipitation of STIM1 and analysis of the immunoprecipitate by western blot using an anti-Prx-4 antibody indicated that Prx-4 is enriched in the anti-STIM1 immunoprecipitate (Fig. 6D).

To investigate the possible role of Prx-4 in regulating the activity of STIM1, experiments were conducted with cultured H4IIE rat liver cells. Prx-4 was knocked down using siRNA, and the effects of decreased Prx-4 expression on SOCE, measured in the presence and absence of H_2O_2, were then assessed. Incubation of H4IIE cells with siRNA targeted against Prx-4 decreased the expression of Prx-4 by 26 ± 4 % (mean ± SEM, n=3) (Fig. 6E). In cells incubated in the absence of H_2O_2, knockdown of Prx-4 did not alter either Ca^{2+} release from the ER, initiated by 2,5-di-(*tert*-butyl)-1,4-benzohydro-quinone (DBHQ), an inhibitor of the ER (Ca^{2+} + Mg^{2+}) ATP-ase [18], or Ca^{2+} entry, initiated by the subsequent addition of extracellular Ca^{2+} (Fig. 7A,C, and E,F). Addition of H_2O_2 to cells pre-treated with negative control siRNA did not inhibit Ca^{2+} release or Ca^{2+} entry (Fig. 7A,B, and E,F). However, addition of H_2O_2 to cells pre-treated with siRNA targeted against Prx-4 inhibited Ca^{2+} entry but did not alter Ca^{2+} release, relative to that in negative control cells (Fig. 7B,D and E,F). In an alternative approach, H4IIE liver cells were treated with Conoidin A, an inhibitor of Prx-4 and of some other peroxiredoxin enzymes [56-58]. The effects of Conoidin A in the presence and absence of H_2O_2 were similar to those observed in cells pre-treated with siRNA targeted against Prx-4 (Fig. 8).

4. Discussion

The aim of this study was to investigate the intracellular distribution of endogenous Orai1 and STIM1in hepatocytes, and to look for novel intracellular STIM1 binding proteins. The strategy employed was to subject the liver to subcellular fractionation then determine the amounts of Orai1 and STIM1 in the major subcellular fractions. The main findings can be summarised as follows. The majority of Orai1 was found in the heavy (44%) and light (27%) microsomal fractions, with only a small proportion (0.03%)in the PM fraction. The majority of STIM1 was found in the heavy microsomal fraction (85%), with some in the light (13%)

microsomal fraction and a small component (0.09%) in the PM fraction. Immunoprecipitation and LC/MS identified Prx-4 as a potential STIM1 binding protein. Knockdown of Prx-4 using siRNA, or inhibition of Prx-4 using conoidin A, did not affect SOCE measured in the absence of H_2O_2, a generator of ROS, but did result in the inhibition of SOCE by H_2O_2.

The conditions of liver homogenisation and differential centrifugation employed in the present study to isolate the heavy and light microsomal and PM fractions were based on those employed previously by others for subcellular fractionation of the liver [23, 28]. The observed distribution of calreticulin and PMCA, markers for the ER and PM, respectively, indicates that there are relatively little PM-derived vesicles in the microsomal fractions while there are some ER-derived vesicles in PM fraction. Hepatocytes comprise about 80% of the cells in the liver [22]. Therefore, it is likely that results for the distribution of STIM1 and Orai1in subcellular fractionations derived from whole liver tissue principally reflect the distribution of Orai1 and STIM1 in hepatocytes, rather than the distribution of these proteins in other cell types present in the liver. Since the PM marker, PMCA, was predominantly located in the PM fraction with little in the microsomal fractions, it is unlikely that the presence of Orai1 in the microsomal fractions is due to contamination of those fractions by large amounts of microsomes derived from the PM.

The observations that Prx-4 was detected in the proteins extracted from heavy microsomes following immunoprecipitation with STIM1, that STIM1 was detected when proteins from the heavy microsomal fraction were subjected to immunoprecipitation using an anti-Prx-4 antibody, and that the enrichment of Prx-4 in the heavy microsomal fraction corresponds to the enrichment of STIM1 in this fraction provide evidence for an association of STIM1 and Prx-4 in the rough ER.

Previous studies have shown that Prx-4 is located in the lumen of the ER where, together with a protein disulphide isomerase and ER oxidoreductase 1, it is thought to

catalyse the conversion of H_2O_2 to H_2O ([51-54]. This pathway, which is responsible for the oxidation of sulphydryl groups on cysteine residues of newly-synthesised proteins to disulphide bonds, is one of the steps in the folding of newly-synthesised proteins [51]. Prx-4 also removes H_2O_2, generated by other oxidase reactions, from the ER lumen [51]. The correct folding of newly-synthesised STIM1 polypeptides may involve the oxidation of two cysteine residues, Cys56 and Cys49 [3]. Several protein disulphide isomerases are involved in protein folding in the ER [51, 59, 60]. One of these isomerases, ERp57, may play an additional role in regulating the activity of STIM1. Thus, it has been shown that the binding of ERp57 to STIM1 inhibits the activation of Orai1 and hence inhibits SOCE [3, 59, 61]. It has also been shown that ROS or H_2O_2 can modify cysteine thiol residues on STIM1 and Orai1 leading to activation of STIM1 and inhibition of Orai1, although interpretation of these results is somewhat complicated (reviewed in [1, 3, 4]).

The present observations that, in liver cells, knockdown of Prx-4 or the inhibition of Prx-4 using Conoidin A [56-58], render SOCE susceptible to inhibition by H_2O_2, a generator of ROS [34], suggests that the functional significance of the interaction of Prx-4 with STIM1 may be to allow Prx-4 to efficiently remove ROS from the vicinity of STIM1, and/or to permit the correct folding of newly-synthesised STIM1. These hypothesised roles of Prx-4 in regulating the activity and/or folding of STIM1 are shown schematically in Fig. 9. While the experiments involving knockdown of Prx-4 or inhibition of Prx-4 were conducted using H4IIE rat liver cells, previous studies have provided evidence that the properties of SOCs in H4IIE cells are similar to those in rat hepatocytes [20].

The observation that, in liver, the majority of endogenous Orai1 was found in microsomes derived from the smooth and rough ER rather than in the PM was somewhat surprising, since functional Orai1 resides in the plasma membrane [1, 14, 16]. Moreover, the

results of many previous experiments conducted with numerous cell types in which ectopic Orai1 tagged with a fluorescent protein such as GFP has been overexpressed have shown that Orai1 is principally located at or near the PM [1, 11, 12, 16]. However, the results of several other studies provide evidence for the internalisation of Orai1 to endosomes, cycling and trafficking of Orai1 between the PM and intracellular organelles, and the location of Orai in acidic organelles including secretory granules [43-45, 62-66]. It is also interesting to note that the distribution of Orai1 amongst the liver subcellular fractions is quite different from that of TRPM2. It is thought that TRPM2 principally functions at the PM, but may also be present in lysosomes, and is also likely to be trafficked to and from the PM [67, 68].

One explanation for the apparent difference between the present results obtained from studying endogenous Orai1 using subcellular fractionation and those obtained from studies of overexpressed ectopic Orai1 in cultured immortalised cells is that, in hepatocytes, Orai1 is located in regions of the rough ER which are close to the PM but which upon homogenisation form heavy microsomes which sediment with the heavy microsomal fraction. A second explanation may be that Orai1 expressed ectopically is trafficked to some intracellular locations which are different from those for endogenous Orai1. The function of Orai1 located in the smooth and rough ER may be to provide a reservoir of Orai1 for insertion into the PM and/or may represent newly-synthesised Orai1 being trafficked to the PM [43, 65]. Another consideration is that, in the present study, the distribution of Orai1 and STIM1 has been studied in subcellular fractions derived from spatially polarised hepatocytes *in situ*, whereas, as mentioned above, many other studies of the intracellular localisation of these proteins have been conducted with cells, often immortalised, in culture.

The observation that the distribution of the secretory granule markers SPCA1 and SPCA2 did not match that of Orai1, suggests that localisation of Orai1 in these organelles does not account for the presence of the bulk of Orai1 observed in the liver microsomal

fractions. However, this does not preclude the presence of some functional Orai1 in secretory granules in hepatocytes, as found in PC12 cells [44].

The majority of STIM1 was found to be located in heavy microsomes derived from the rough ER with little in the PM fraction. This distribution is broadly consistent with the results of previous studies on the distribution of endogenous STIM1 in K562 cells and in HEK 293 cells [69, 70]. STIM1 polypeptides involved in the activation of Orai1 at PM-ER junctions would be expected to reside and function in the smooth ER at the periphery of the cell adjacent to the PM [1, 13, 15]. Several previous studies have provided evidence that bulky ribosomes attached to the rough ER would prevent the ER from coming sufficiently close to the PM in a PM-ER junction so that STIM1 polypeptides can interact with Orai1 polypeptides [5, 6]. The amount of cortical ER involved in PM-ER junctions is likely to be a very small proportion of the total in the ER. This raises the question of the likely function of STIM1 located in the rough ER. This presumably does not participate directly in the activation of Orai1. However, STIM1 located in the rough ER may provide a reservoir of STIM1 for supply to the cortical ER, may regulate other functions of the ER independent of interaction with Orai1, and may be involved in the regulation of microtubule formation and remodelling of the ER [8-10, 71, 72].

Treatment with phenylephrine to release Ca^{2+} from intracellular stores and activate SOCE did not cause a detectable change in the distribution of Orai1 and STIM1 between subcellular fractions. There is some evidence to indicate that the activation of Orai1, and hence SOCE, by STIM1 may involve an increase in the amounts of Orai1 and/or STIM1 in the PM (reviewed by Prakriya and Lewis [1]). However, such a redistribution of STIM1 and Orai1 is likely to involve a very small fraction of the total amounts of these proteins present in the hepatocyte and would not be detected in the present study of subcellular fractions. In some cell types the release of Ca^{2+} from the ER induced by the SERCA inhibitor thapsigargin

is associated with the trafficking of significant amounts of Orai1 to the PM [43, 73]. It is possible that in hepatocytes *in situ*, pre-treatment with thapsigargin leads to a much larger release of ER Ca^{2+} than that induced by phenylephrine, the hormone analogue employed in the present study. This may, in turn, cause a larger increase in Orai1 in the PM fraction, which might have been detectable using the subcellar fractionation approach employed in this study. Indeed, many other conditions, such as steatosis or drug-induced liver toxicity, are known to cause ER stress and an increase in ROS in hepatocytes [18, 34, 74]. These may also cause a larger release of ER Ca^{2+} than that initiated by phenylephrine and may also cause an increase the amount of Orai1 in the PM fraction which would be detectable by the subcellular fractionation approach.

The association of Prx-4 with STIM1 may also affect the activity and intracellular distribution of Orai1. A relationship between the concentration of ROS, Orai1, and SOCE has been reported in mast cells [75]. In the present study, the experiments to investigate the role of Prx-4 in the regulation of SOCE were conducted using H4IIE rat liver cells in culture. Under these cell culture conditions, some of the cells are proliferating, the concentration of ROS may be elevated, and ER Ca^{2+} may be partly depleted. Studies of the intracellular distribution of Orai1 and STIM1 were conducted using homogenates of rat liver where the majority of hepatocytes are quiescent and the concentration of ROS within hepatocytes is likely low. It is possible that in H4IIE cells in culture more Orai1 may be located at the PM than in quiescent hepatocytes, leading to greater Ca^{2+} entry via SOCE. Further studies to compare the trafficking of Orai1 to the PM and the amount of Orai1 in the PM in both quiescent hepatocytes *in situ* and in proliferating H4IIE cells in culture under conditions of elevated ROS and ER stress are warranted.

It is concluded that, in hepatocytes *in situ*, a considerable proportion of endogenous Orai1 and STIM1 is located in the ER. Orai1 present in the ER may be close to the PM where it may provide a reservoir of Orai1 for insertion into the PM as part of the cycling of Orai1 between the PM and ER in the regulation of SOCE. STIM1 present in the ER may be involved in processes independent of SOCE, such as the regulation of microtubules, and may also represent STIM1 being trafficked to the PM. In addition, STIM1 interacts with Prx-4, and this interaction may contribute to the regulation of STIM1 and SOCE by ROS.

Funding

This study was supported by grants from the Australian Research Council (DP140100259), National Health and Medical Research Council (519115), Flinders University, and the Flinders Medical Centre Foundation.

Conflict of Interest Statement

We wish to confirm that there are no known conflicts of interest associated with this publication and there has been no significant financial support for this work that could have influenced its outcome.

Acknowledgements

Advice provided by Dr. Yabin Zhou and Nusha Chegeni, Flinders University, Adelaide; and Dr Sarah Ho, Hong Kong University of Science and Technology, Hong Kong, is gratefully acknowledged.

References

[1] M. Prakriya, R.S. Lewis, Store-Operated Calcium Channels, Physiological reviews, 95 (2015) 1383-1436.
[2] D.M. Cooper, Store-operated Ca(2)(+)-entry and adenylyl cyclase, Cell Calcium, 58 (2015) 368-375.
[3] P. Nunes, N. Demaurex, Redox regulation of store-operated Ca2+ entry, Antioxidants & redox signaling, 21 (2014) 915-932.
[4] R. Bhardwaj, M.A. Hediger, N. Demaurex, Redox modulation of STIM-ORAI signaling, Cell Calcium, 60 (2016) 142-152.
[5] G. Lur, L.P. Haynes, I.A. Prior, O.V. Gerasimenko, S. Feske, O.H. Petersen, R.D. Burgoyne, A.V. Tepikin, Ribosome-free terminals of rough ER allow formation of STIM1 puncta and segregation of STIM1 from IP(3) receptors, Curr Biol, 19 (2009) 1648-1653.
[6] L. Orci, M. Ravazzola, M. Le Coadic, W.W. Shen, N. Demaurex, P. Cosson, STIM1-induced precortical and cortical subdomains of the endoplasmic reticulum, Proceedings of the National Academy of Sciences of the United States of America, 106 (2009) 19358-19362.
[7] N.R. Scrimgeour, D.P. Wilson, G.J. Barritt, G.Y. Rychkov, Structural and stoichiometric determinants of Ca2+ release-activated Ca2+ (CRAC) channel Ca2+-dependent inactivation, Biochimica et biophysica acta, 1838 (2014) 1281-1287.
[8] R. Hooper, E. Samakai, J. Kedra, J. Soboloff, Multifaceted roles of STIM proteins, Pflugers Archiv : European journal of physiology, 465 (2013) 1383-1396.
[9] W.W. Shen, M. Frieden, N. Demaurex, Remodelling of the endoplasmic reticulum during store-operated calcium entry, Biol Cell, 103 (2011) 365-380.
[10] J.T. Smyth, W.I. DeHaven, G.S. Bird, J.W. Putney, Jr., Role of the microtubule cytoskeleton in the function of the store-operated Ca2+ channel activator STIM1, Journal of cell science, 120 (2007) 3762-3771.
[11] V.A. Barr, K.M. Bernot, S. Srikanth, Y. Gwack, L. Balagopalan, C.K. Regan, D.J. Helman, C.L. Sommers, M. Oh-Hora, A. Rao, L.E. Samelson, Dynamic movement of the calcium sensor STIM1 and the calcium channel Orai1 in activated T-cells: puncta and distal caps, Mol Biol Cell, 19 (2008) 2802-2817.
[12] M. Chvanov, C.M. Walsh, L.P. Haynes, S.G. Voronina, G. Lur, O.V. Gerasimenko, R. Barraclough, P.S. Rudland, O.H. Petersen, R.D. Burgoyne, A.V. Tepikin, ATP depletion induces translocation of STIM1 to puncta and formation of STIM1-ORAI1 clusters: translocation and re-translocation of STIM1 does not require ATP, Pflugers Archiv : European journal of physiology, 457 (2008) 505-517.
[13] J.T. Smyth, W.I. Dehaven, G.S. Bird, J.W.J. Putney, Ca2+-store-dependent and -independent reversal of Stim1 localization and function, Journal of cell science, 121 (2008) 762-772.
[14] R.M. Luik, M.M. Wu, J. Buchanan, R.S. Lewis, The elementary unit of store-operated Ca2+ entry: local activation of CRAC channels by STIM1 at ER-plasma membrane junctions, Journal of Cell Biology, 174 (2006) 815-825.
[15] M.M. Wu, J. Buchanan, R.M. Luik, R.S. Lewis, Ca2+ store depletion causes STIM1 to accumulate in ER regions closely associated with the plasma membrane, Journal of Cell Biology, 174 (2006) 803-813.

[16] Y. Gwack, S. Srikanth, S. Feske, F. Cruz-Guilloty, M. Oh-hora, D.S. Neems, P.G. Hogan, A. Rao, Biochemical and functional characterization of Orai proteins, J Biol Chem, 282 (2007) 16232-16243.
[17] G. Rychkov, H.M. Brereton, M.L. Harland, G.J. Barritt, Plasma membrane Ca2+ release-activated Ca2+ channels with a high selectivity for Ca2+ identified by patch-clamp recording in rat liver cells, Hepatology, 33 (2001) 938-947.
[18] C.H. Wilson, E.S. Ali, N. Scrimgeour, A.M. Martin, J. Hua, G.A. Tallis, G.Y. Rychkov, G.J. Barritt, Steatosis inhibits liver cell store-operated Ca(2)(+) entry and reduces ER Ca(2)(+) through a protein kinase C-dependent mechanism, Biochem J, 466 (2015) 379-390.
[19] G.Y. Rychkov, T. Litjens, M.L. Roberts, G.J. Barritt, ATP and vasopressin activate a single type of store-operated Ca2+ channel, identified by patch-clamp recording, in rat hepatocytes, Cell Calcium, 37 (2005) 183-191.
[20] E.C. Aromataris, J. Castro, G. Rychkov, G.J. Barritt, Store-operated Ca2+ channels and Stromal Interaction Molecule 1 (STIM1) are targets for the actions of bile acids on liver cells, Biochimica et Biophysica Acta - Molecular Cell Research, 1783 (2008) 874-885.
[21] J. Castro, E.C. Aromataris, G.Y. Rychkov, G.J. Barritt, A small component of the endoplasmic reticulum is required for store-operated Ca2+ channel activation in liver cells: evidence from studies using TRPV1 and taurodeoxycholic acid, Biochem J, 418 (2009) 553-566.
[22] B. Young, J.W. Heath, Liver and Pancreas, Wheater's Functional Histology, Churchill Livingstone, Edinburgh, 2000, pp. 274-275.
[23] A. Amar-Costesec, H. Beaufay, M. Wibo, D. Thines-Sempoux, E. Feytmans, M. Robbi, J. Berthet, Analytical study of microsomes and isolated subcellular membranes from rat liver. II. Preparation and composition of the microsomal fraction, The Journal of cell biology, 61 (1974) 201-212.
[24] J.H. Cox, S. Hussell, H. Sondergaard, K. Roepstorff, J.V. Bui, J.R. Deer, J. Zhang, Z.G. Li, K. Lamberth, P.H. Kvist, S. Padkjaer, C. Haase, S. Zahn, V.H. Odegard, Antibody-mediated targeting of the Orai1 calcium channel inhibits T cell function, PLoS One, 8 (2013) e82944.
[25] H.L. Ong, J. Chen, T. Chataway, H. Brereton, L. Zhang, T. Downs, L. Tsiokas, G. Barritt, Specific detection of the endogenous transient receptor potential (TRP)-1 protein in liver and airway smooth muscle cells using immunoprecipitation and Western-blot analysis, Biochemical Journal 364 (2002) 641-648.
[26] T. Litjens, T. Nguyen, J. Castro, E.C. Aromataris, L. Jones, G.J. Barritt, G.Y. Rychkov, Phospholipase C-gamma1 is required for the activation of store-operated Ca2+ channels in liver cells, Biochem J, 405 (2007) 269-276.
[27] C. Wilson, S. Zeile, T. Chataway, V.B. Nieuwenhuijs, R.T.A. Padbury, G.J. Barritt, Increased expression of peroxiredoxin 1 and a novel lipid metabolising enzyme in the early phase of liver ischemia reperfusion injury, Proteomics, (2011).
[28] J.-P. Lievremont, A.-M. Hill, M. Hilly, J.-P. Mauger, The inositol 1,4,5-trisphosphate receptor is localised on specialised sub-regions of the endoplasmic reticulum in rat liver, Biochem J 300 (1994) 419-427.
[29] V. Prpic, K.C. Green, P.F. Blackmore, J.H. Exton, Vasopressin-, angiotensin II-, and alpha 1-adrenergic-induced inhibition of Ca2+ transport by rat liver plasma membrane vesicles, J Biol Chem, 259 (1984) 1382-1385.
[30] B.J. Agnew, D. Murray, W.F. Patton, A rapid solid-phase fluorescence-based protein assay for quantitation of protein electrophoresis samples containing detergents, chaotropes, dyes, and reducing agents, Electrophoresis, 25 (2004) 2478-2485.

[31] N.B. Argent, J. Liles, D. Rodham, C.B. Clayton, R. Wilkinson, P.H. Baylis, A new method for measuring the blood volume of the rat using 113mIndium as a tracer, Lab Anim, 28 (1994) 172-175.
[32] R. Naderi, A. Imani, M. Faghihi, M. Moghimian, Phenylephrine induces early and late cardioprotection through mitochondrial permeability transition pore in the isolated rat heart, J Surg Res, 164 (2010) e37-42.
[33] E.C. Aromataris, M.L. Roberts, G.J. Barritt, G.Y. Rychkov, Glucagon activates Ca2+ and Cl- channels in rat hepatocytes, J Physiol (Lond), 573 (2006) 611-625.
[34] E. Kheradpezhouh, L. Ma, A. Morphett, G.J. Barritt, G.Y. Rychkov, TRPM2 channels mediate acetaminophen-induced liver damage, Proceedings of the National Academy of Sciences of the United States of America, 111 (2014) 3176-3181.
[35] G. Grynkiewicz, M. Poenie, R.Y. Tsien, A new generation of Ca2+ indicators with greatly improved fluorescence properties, J Biol Chem, 260 (1985) 3440-3450.
[36] M.J. Smith, G.L. Koch, Multiple zones in the sequence of calreticulin (CRP55, calregulin, HACBP), a major calcium binding ER/SR protein, EMBO J, 8 (1989) 3581-3586.
[37] H. Hilfiker, D. Guerini, E. Carafoli, Cloning and expression of isoform 2 of the human plasma membrane Ca2+ ATPase. Functional properties of the enzyme and its splicing products, J Biol Chem, 269 (1994) 26178-26183.
[38] F. Kessler, F. Bennardini, O. Bachs, J. Serratosa, P. James, A.J. Caride, P. Gazzotti, J.T. Penniston, E. Carafoli, Partial purification and characterization of the Ca2(+)-pumping ATPase of the liver plasma membrane, J Biol Chem, 265 (1990) 16012-16019.
[39] N. Tolosa de Talamoni, C.A. Smith, R.H. Wasserman, C. Beltramino, C.S. Fullmer, J.T. Penniston, Immunocytochemical localization of the plasma membrane calcium pump, calbindin-D28k, and parvalbumin in Purkinje cells of avian and mammalian cerebellum, Proceedings of the National Academy of Sciences of the United States of America, 90 (1993) 11949-11953.
[40] I. Garcia-Arcos, Y. Rueda, P. Gonzalez-Kother, L. Palacios, B. Ochoa, O. Fresnedo, Association of SND1 protein to low density lipid droplets in liver steatosis, J Physiol Biochem, 66 (2010) 73-83.
[41] R. Guzman, E.G. Valente, J. Pretorius, E. Pacheco, M. Qi, B.D. Bennett, D.H. Fong, F.F. Lin, V. Bi, H.J. McBride, Expression of ORAII, a plasma membrane resident subunit of the CRAC channel, in rodent and non-rodent species, J Histochem Cytochem, 62 (2014) 864-878.
[42] H. Balghi, R. Robert, B. Rappaz, X. Zhang, A. Wohlhuter-Haddad, A. Evagelidis, Y. Luo, J. Goepp, P. Ferraro, P. Romeo, M. Trebak, P.W. Wiseman, D.Y. Thomas, J.W. Hanrahan, Enhanced Ca2+ entry due to Orai1 plasma membrane insertion increases IL-8 secretion by cystic fibrosis airways, FASEB journal : official publication of the Federation of American Societies for Experimental Biology, 25 (2011) 4274-4291.
[43] G.E. Woodard, G.M. Salido, J.A. Rosado, Enhanced exocytotic-like insertion of Orai1 into the plasma membrane upon intracellular Ca2+ store depletion, American journal of physiology. Cell physiology, 294 (2008) C1323-1331.
[44] E.J. Dickson, J.G. Duman, M.W. Moody, L. Chen, B. Hille, Orai-STIM-mediated Ca2+ release from secretory granules revealed by a targeted Ca2+ and pH probe, Proceedings of the National Academy of Sciences of the United States of America, 109 (2012) E3539-3548.
[45] H. Zbidi, I. Jardin, G.E. Woodard, J.J. Lopez, A. Berna-Erro, G.M. Salido, J.A. Rosado, STIM1 and STIM2 are located in the acidic Ca2+ stores and associates with Orai1 upon depletion of the acidic stores in human platelets, J Biol Chem, 286 (2011) 12257-12270.
[46] P.H. Reinhart, W.M. Taylor, F.L. Bygrave, Calcium ion fluxes induced by the action of alpha-adrenergic agonists in perfused rat liver, Biochem J, 208 (1982) 619-630.

[47] D.A. Hems, P.D. Whitton, G.Y. Ma, Metabolic actions of vasopressin, glucagon and adrenalin in the intact rat, Biochimica et biophysica acta, 411 (1975) 155-164.
[48] J.K. Saha, J. Xia, J.M. Grondin, S.K. Engle, J.A. Jakubowski, Acute hyperglycemia induced by ketamine/xylazine anesthesia in rats: mechanisms and implications for preclinical models, Exp Biol Med (Maywood), 230 (2005) 777-784.
[49] K. Hodge, S.T. Have, L. Hutton, A.I. Lamond, Cleaning up the masses: exclusion lists to reduce contamination with HPLC-MS/MS, J Proteomics, 88 (2013) 92-103.
[50] L. Trinkle-Mulcahy, S. Boulon, Y.W. Lam, R. Urcia, F.M. Boisvert, F. Vandermoere, N.A. Morrice, S. Swift, U. Rothbauer, H. Leonhardt, A. Lamond, Identifying specific protein interaction partners using quantitative mass spectrometry and bead proteomes, The Journal of cell biology, 183 (2008) 223-239.
[51] S.G. Rhee, H.A. Woo, I.S. Kil, S.H. Bae, Peroxiredoxin functions as a peroxidase and a regulator and sensor of local peroxides, J Biol Chem, 287 (2012) 4403-4410.
[52] E. Zito, PRDX4, an endoplasmic reticulum-localized peroxiredoxin at the crossroads between enzymatic oxidative protein folding and nonenzymatic protein oxidation, Antioxidants & redox signaling, 18 (2013) 1666-1674.
[53] E. Zito, E.P. Melo, Y. Yang, A. Wahlander, T.A. Neubert, D. Ron, Oxidative protein folding by an endoplasmic reticulum-localized peroxiredoxin, Mol Cell, 40 (2010) 787-797.
[54] T.J. Tavender, J.J. Springate, N.J. Bulleid, Recycling of peroxiredoxin IV provides a novel pathway for disulphide formation in the endoplasmic reticulum, EMBO J, 29 (2010) 4185-4197.
[55] Y. Sato, R. Kojima, M. Okumura, M. Hagiwara, S. Masui, K. Maegawa, M. Saiki, T. Horibe, M. Suzuki, K. Inaba, Synergistic cooperation of PDI family members in peroxiredoxin 4-driven oxidative protein folding, Sci Rep, 3 (2013) 2456.
[56] J.D. Haraldsen, G. Liu, C.H. Botting, J.G. Walton, J. Storm, T.J. Phalen, L.Y. Kwok, D. Soldati-Favre, N.H. Heintz, S. Muller, N.J. Westwood, G.E. Ward, Identification of Conoidin a as a Covalent Inhibitor of Peroxiredoxin Ii, Org Biomol Chem, 7 (2009) 3040-3048.
[57] G. Liu, C.H. Botting, K.M. Evans, J.A. Walton, G. Xu, A.M. Slawin, N.J. Westwood, Optimisation of conoidin A, a peroxiredoxin inhibitor, ChemMedChem, 5 (2010) 41-45.
[58] J.B. Nguyen, C.D. Pool, C.Y. Wong, R.S. Treger, D.L. Williams, M. Cappello, W.A. Lea, A. Simeonov, J.J. Vermeire, Y. Modis, Peroxiredoxin-1 from the human hookworm Ancylostoma ceylanicum forms a stable oxidized decamer and is covalently inhibited by conoidin A, Chem Biol, 20 (2013) 991-1001.
[59] A. Hettinghouse, R. Liu, C.J. Liu, Multifunctional molecule ERp57: From cancer to neurodegenerative diseases, Pharmacol Ther, 181 (2018) 34-48.
[60] C.E. Jessop, R.H. Watkins, J.J. Simmons, M. Tasab, N.J. Bulleid, Protein disulphide isomerase family members show distinct substrate specificity: P5 is targeted to BiP client proteins, Journal of cell science, 122 (2009) 4287-4295.
[61] D. Prins, J. Groenendyk, N. Touret, M. Michalak, Modulation of STIM1 and capacitative Ca2+ entry by the endoplasmic reticulum luminal oxidoreductase ERp57, EMBO Rep, 12 (2011) 1182-1188.
[62] A. Bohorquez-Hernandez, E. Gratton, J. Pacheco, A. Asanov, L. Vaca, Cholesterol modulates the cellular localization of Orai1 channels and its disposition among membrane domains, Biochimica et biophysica acta, 1862 (2017) 1481-1490.
[63] J.T. Smyth, J.W. Putney, Regulation of store-operated calcium entry during cell division, Biochem Soc Trans, 40 (2012) 119-123.
[64] F. Yu, L. Sun, K. Machaca, Orai1 internalization and STIM1 clustering inhibition modulate SOCE inactivation during meiosis, Proceedings of the National Academy of Sciences of the United States of America, 106 (2009) 17401-17406.

[65] F. Yu, L. Sun, K. Machaca, Constitutive recycling of the store-operated Ca2+ channel Orai1 and its internalization during meiosis, The Journal of cell biology, 191 (2010) 523-535.
[66] B. Zeng, G.L. Chen, E. Garcia-Vaz, S. Bhandari, N. Daskoulidou, L.M. Berglund, H. Jiang, T. Hallett, L.P. Zhou, L. Huang, Z.H. Xu, V. Nair, R.G. Nelson, W. Ju, M. Kretzler, S.L. Atkin, M.F. Gomez, S.Z. Xu, ORAI channels are critical for receptor-mediated endocytosis of albumin, Nat Commun, 8 (2017) 1920.
[67] T.K. Kim, J.H. Nam, W.G. Ahn, N.H. Kim, H.Y. Ham, C.W. Hong, J.S. Nam, J. Lee, S.O. Huh, I. So, S.J. Kim, D.K. Song, Lys1110 of TRPM2 is critical for channel activation, Biochem J, 455 (2013) 319-327.
[68] F. Li, N. Abuarab, A. Sivaprasadarao, Reciprocal regulation of actin cytoskeleton remodelling and cell migration by Ca2+ and Zn2+: role of TRPM2 channels, Journal of cell science, 129 (2016) 2016-2029.
[69] S.S. Manji, N.J. Parker, R.T. Williams, L. van Stekelenburg, R.B. Pearson, M. Dziadek, P.J. Smith, STIM1: a novel phosphoprotein located at the cell surface, Biochimica et biophysica acta, 1481 (2000) 147-155.
[70] O. Mignen, J.L. Thompson, T.J. Shuttleworth, STIM1 regulates Ca2+ entry via arachidonate-regulated Ca2+-selective (ARC) channels without store depletion or translocation to the plasma membrane, J Physiol, 579 (2007) 703-715.
[71] I. Grigoriev, S.M. Gouveia, B. van der Vaart, J. Demmers, J.T. Smyth, S. Honnappa, D. Splinter, M.O. Steinmetz, J.W. Putney, Jr., C.C. Hoogenraad, A. Akhmanova, STIM1 is a MT-plus-end-tracking protein involved in remodeling of the ER, Curr Biol, 18 (2008) 177-182.
[72] S. Maschalidi, P. Nunes-Hasler, C.R. Nascimento, I. Sallent, V. Lannoy, M. Garfa-Traore, N. Cagnard, F.E. Sepulveda, P. Vargas, A.M. Lennon-Dumenil, P. van Endert, T. Capiod, N. Demaurex, G. Darrasse-Jeze, B. Manoury, UNC93B1 interacts with the calcium sensor STIM1 for efficient antigen cross-presentation in dendritic cells, Nat Commun, 8 (2017) 1640.
[73] R. Hodeify, S. Selvaraj, J. Wen, A. Arredouani, S. Hubrack, M. Dib, S.N. Al-Thani, T. McGraw, K. Machaca, A STIM1-dependent 'trafficking trap' mechanism regulates Orai1 plasma membrane residence and Ca(2)(+) influx levels, Journal of cell science, 128 (2015) 3143-3154.
[74] S.W. Park, Y. Zhou, J. Lee, U. Ozcan, Sarco(endo)plasmic reticulum Ca2+-ATPase 2b is a major regulator of endoplasmic reticulum stress and glucose homeostasis in obesity, Proceedings of the National Academy of Sciences of the United States of America, 107 (2010) 19320-19325.
[75] B. Yang, C. Yang, P. Wang, J. Li, H. Huang, Q. Ji, J. Liu, Z. Liu, Food allergen--induced mast cell degranulation is dependent on PI3K-mediated reactive oxygen species production and upregulation of store-operated calcium channel subunits, Scand J Immunol, 78 (2013) 35-43.
[76] P. Lai, F. Michelangeli, Bis(2-hydroxy-3-tert-butyl-5-methyl-phenyl)-methane (bis-phenol) is a potent and selective inhibitor of the secretory pathway Ca(2)(+) ATPase (SPCA1), Biochemical and biophysical research communications, 424 (2012) 616-619.

Legends to Figures

Fig. 1. Western blot images for calreticulin, plasma membrane (Ca^{2+} + Mg^{2+})ATP-ase, STIM1 and Orai1 in microsomal fractions derived from the endoplasmic reticulum and plasma membrane, showing linearity of band intensity with amount of protein applied to the gel. Each panel shows the western blot image for a range of amounts of protein applied to each lane (indicated below the lane) and a plot of band intensity as a function of amount of protein applied to the gel for calreticulin (A), plasma membrane (Ca^{2+} + Mg^{2+})ATP-ase (PMCA) (B), STIM1 (C) and Orai1 (D). The subcellular fractions subject to western blot were the heavy microsomal fraction (A-C) and PM fraction (D). The results are the means ± SEM obtained from the analysis of 4-5 western blots. The lines were drawn on the basis of a linear regression analysis. The entire western blot images are shown in Supplemental Data Fig. S1.

Fig. 2. Distribution of calreticulin and plasma membrane (Ca^{2+} + Mg^{2+})ATP-ase in subcellular fractions of untreated rat liver. A,B. Western blot images showing calreticulin (Cal) (50 kDa) and (Ca^{2+} + Mg^{2+})ATP-ase (PMCA) (150 kDa) in whole liver and in subcellular fractions derived from the "Plasma Membrane and Microsomal Fractionation" (A) and the "Mitochondria, Microsomal and Cytosolic Fractionation" (B). WL, whole liver; LSP, low speed pellet; Mit, mitochondria; HM, heavy microsomes; LM light microsomes; and Cyt, cytosol. The images shown are representative of those obtained in 4-6 experiments. C-E. Enrichment of calreticulin (C,D) and PMCA (E) in subcellular fractions from the "Plasma Membrane and Microsomal Fractionation" (C and E) and the "Mitochondria, Microsomal and Cytosolic Fractionation" (D). The "Plasma Membrane and Microsomal Fractionation" and the "Mitochondria, Microsomal and Cytosolic Fractionation" were conducted as described in Materials and methods. Results, expressed as band intensity (arbitrary units) per mg protein, are the means ± SEM obtained from the analysis western

blots of subcellular fractions derived from 4-6 separate livers. Degrees of significance in C, D and E for comparison of band intensity in a given subcellular fraction with that in WL are: * $P<0.05$, ** $P<0.01$, and *** $P<0.001$. The entire western blot images are shown in Supplemental Data Fig. S2.

Fig. 3. Distribution of STIM1 in subcellular fractions of rat liver. A. Western blots showing STIM1 (75 kDa) in whole liver and in subcellular fractions derived from the "Plasma Membrane and Microsomal Fractionation" (upper panel) and the "Mitochondria, Microsomal and Cytosolic Fractionation" (lower panel) of untreated and phenylephrine-treated livers. WL, whole liver; LSP, low speed pellet; Mit, mitochondria; HM, heavy microsomes; LM light microsomes; and Cyt, cytosol. The images shown are representative of those obtained in 4-7 experiments. B,C Enrichment of STIM1 in subcellular fractions derived from the "Plasma Membrane and Microsomal Fractionation" (B) and the "Mitochondria, Microsomal and Cytosolic Fractionation" (C) from untreated and phenylephrine-treated livers. The "Plasma Membrane and Microsomal Fractionation" and the "Mitochondria, Microsomal and Cytosolic Fractionation" were conducted as described in Materials and methods. Results, expressed as band intensity (arbitrary units) per mg protein, are the means ± SEM obtained from western blots of subcellular fractions derived from 4-7 separate livers. Degrees of significance for comparison of band intensity in a given subcellular fraction with that in WL are: * $P<0.05$. The entire western blot images are shown in Supplemental Data Fig. S3.

Fig. 4. Distribution of Orai1 in subcellular fractions of rat liver. A. Western blot showing Orai1 (45 kDa) in whole liver and in subcellular fractions derived from the "Plasma Membrane and Microsomal Fractionation" of untreated liver. WL, whole liver; HM, heavy microsomes; and LM, light microsomes. The image shown is representative of those obtained

in 4-6 experiments. B. Enrichment of Orai1 in subcellular fractions derived from the "Plasma Membrane and Microsomal Fractionation" of untreated and phenylephrine-treated livers. The "Plasma Membrane and Microsomal Fractionation" and the "Mitochondria, Microsomal and Cytosolic Fractionation" were conducted as described in Materials and methods. Results, expressed as band intensity (arbitrary units) per mg protein, are the means ± SEM obtained from western blots of subcellular fractions derived from 4-7 separate livers. Degrees of significance in B for comparison of band intensity in a given subcellular fraction with that in WL are: * $P<0.05$, and ** $P<0.01$. The entire western blot image is shown in Supplemental Data Fig. S4.

Fig. 5. Distribution of TRPM2 and Ca^{2+} ATP-ases 1 and 2 in subcellular fractions of rat liver. A. Western blot showing TRPM2 (150 kDa) in whole liver and in subcellular fractions derived from the "Mitochondria, Microsomal and Cytosolic Fractionation" of untreated livers. WL, whole liver; LSP, low speed pellet; Mit, mitochondria; HM, heavy microsomes; LM light microsomes; and Cyt, cytosol. The image shown is representative of that obtained in one of three experiments. B. Enrichment of TRPM2 in subcellular fractions derived from the "Mitochondria, Microsomal and Cytosolic Fractionation" from untreated livers. The results are expressed as intensity (arbitrary units) of the TRPM2 150 kDa band for a given subcellular fraction (30 μg protein per lane) and are the means ± SEM obtained from western blots of subcellular fractions derived from 3 separate livers. C. Western blot showing SPCA1 (about 100 kDa) and SPCA2 (about 110 kDa) in subcellular fractions derived from the "Mitochondria, Microsomal and Cytosolic Fractionation" of untreated liver. HM, heavy microsomes; LM, light microsomes and Cyt, cytosol. The "Mitochondria, Microsomal and Cytosolic Fractionation" was conducted as described in Materials and methods. The images shown are representative of those obtained in three experiments. Degrees of significance in B

for comparison of band intensity in a given subcellular fraction with that in WL are: ** $P<0.01$.

Fig. 6. Immunoprecipitation of STIM1 from the heavy microsomal fraction and identification of peroxiredoxin-4 in the immunoprecipitate. A. Western blot of STIM1 (75 kDa) in the precipitate resulting from the immunoprecipitation of STIM1 from the heavy microsomal subcellular fraction prepared from untreated livers. STIM1 was immunoprecipitated using an anti-STIM1 antibody (Abcam, # 52458), and identified in the western blot using the same anti-STIM1 antibody. B. Western blot identifying peroxiredoxin-4 (Prx-4) (monomer 25 kDa and dimer 50 kDa) in in whole liver (WL) and the low speed pellet (LSP), mitochondrial (Mt), heavy microsomal (HM), light microsomal (LM) and cytosolic (Cyt) subcellular fractions. C. Enrichment of Prx-4 in subcellular fractions derived from the "Mitochondria, Microsomal and Cytosolic Fractionation" from untreated livers. LSP, low speed pellet. Results are expressed as the sum of the intensities of the 25 and 50 kDa bands (arbitrary units of band intensity for 30 μg protein applied per lane), relative to that of the band for whole liver, and are the means ± SEM obtained from western blots of subcellular fractions derived from three separate livers. D. Western blot of Prx-4 (25 and 50 kDa) in the precipitate resulting from the immunoprecipitation of STIM1 from the heavy microsomal subcellular fraction prepared from untreated livers. STIM1 was immunoprecipitated (anti-STIM1 antibody Abcam, # 52458) and Prx-4 detected using anti-Prx-4 antibody (Biosensis, # R-1593-100). E. Knockdown of Prx-4 using siRNA targeted against Prx-4 in H4IIE rat liver cells. The amount of protein added to each lane for control cells (No siRNA), cells incubated with scrambled siRNA (siCtl) and with siRNA targeted against Prx-4 (siPrx-4) is indicated under each lane. Quantitation of band intensities gave values of 79, 77, and 80 % for the intensity of the band for siPrx-4 as a percentage of that for siCtl for 2.0, 5.0 and 10.0 μg

protein per lane, respectively. The western blot images in A,B and D and E are representative of those obtained in three experiments which each gave similar results. Degrees of significance in C for comparison of band intensity in a given subcellular fraction with that in WL, and for comparison of HM with LM, are: * $P<0.05$ and *** $P<0.001$.

Fig. 7. Effects of knockdown of Prx-4 on store-operated Ca^{2+} entry measured in the absence and presence of hydrogen peroxide. A-D. Representative traces showing the effects of the addition of DBHQ in the absence of added extracellular Ca^{2+} (Ca^{2+}_{ext}) and the subsequent addition of 2.4 mM Ca^{2+}_{ext} on $[Ca^{2+}]_{cyt}$, in H4IIE rat liver cells incubated with scrambled siRNA (Control siRNA) (A,B) or siRNA targeted against Prx-4 (Prx-4 siRNA) (C,D) in the absence (A,C) and presence (B,D) of H_2O_2. E,F. Amounts of Ca^{2+} released by DBHQ (peak height), and initial rates of Ca^{2+} entry following Ca^{2+}_{ext} addition, respectively (means ± SEM (n = 3 independent experiments)). Degrees of significance: *$P<0.05$.

Fig. 8. Effects of Conoidin A, an inhibitor of Prx-4, on store-operated Ca^{2+} entry measured in the absence and presence of hydrogen peroxide. A-D. Representative traces showing the effects of the addition of DBHQ in the absence of added extracellular Ca^{2+} (Ca^{2+}_{ext}) and the subsequent addition of 2.4 mM Ca^{2+}_{ext} on $[Ca^{2+}]_{cyt}$, in H4IIE rat liver cells pre-incubated for 24 h in the absence (A,B) or presence (C,D) of 50 μM Conoidin A, and in the absence (A,C) and presence (B,D) of H_2O_2. E,F. Amounts of Ca^{2+} released by DBHQ (peak height), and initial rates of Ca^{2+} entry following Ca^{2+}_{ext} addition, respectively (means ± SEM (n = 3 independent experiments)). Degrees of significance: **$P<0.01$.

Fig. 9. Schematic representation of the hypothesised role(s) of peroxiredoxin-4 (Prx4) in regulating the activation of store-operated Ca^{2+} entry in hepatocytes. Following the release of Ca^{2+} from the cEF binding site of STIM1 in the lumen of the ER, and subsequent changes in conformation, STIM1 interacts with Orai1 and activates the SOCE [1]. It is hypothesised that Prx-4 binds to STIM1 and may regulate the folding of STIM1 in the ER (1) and/or may simply remove ROS and prevent ROS-induced inhibition of STIM1 (2). PDI, protein disulphide isomerase; Ero1, ER oxidoreductase; Prx-4, peroxiredoxin-4. Scheme based on [4, 54, 61].

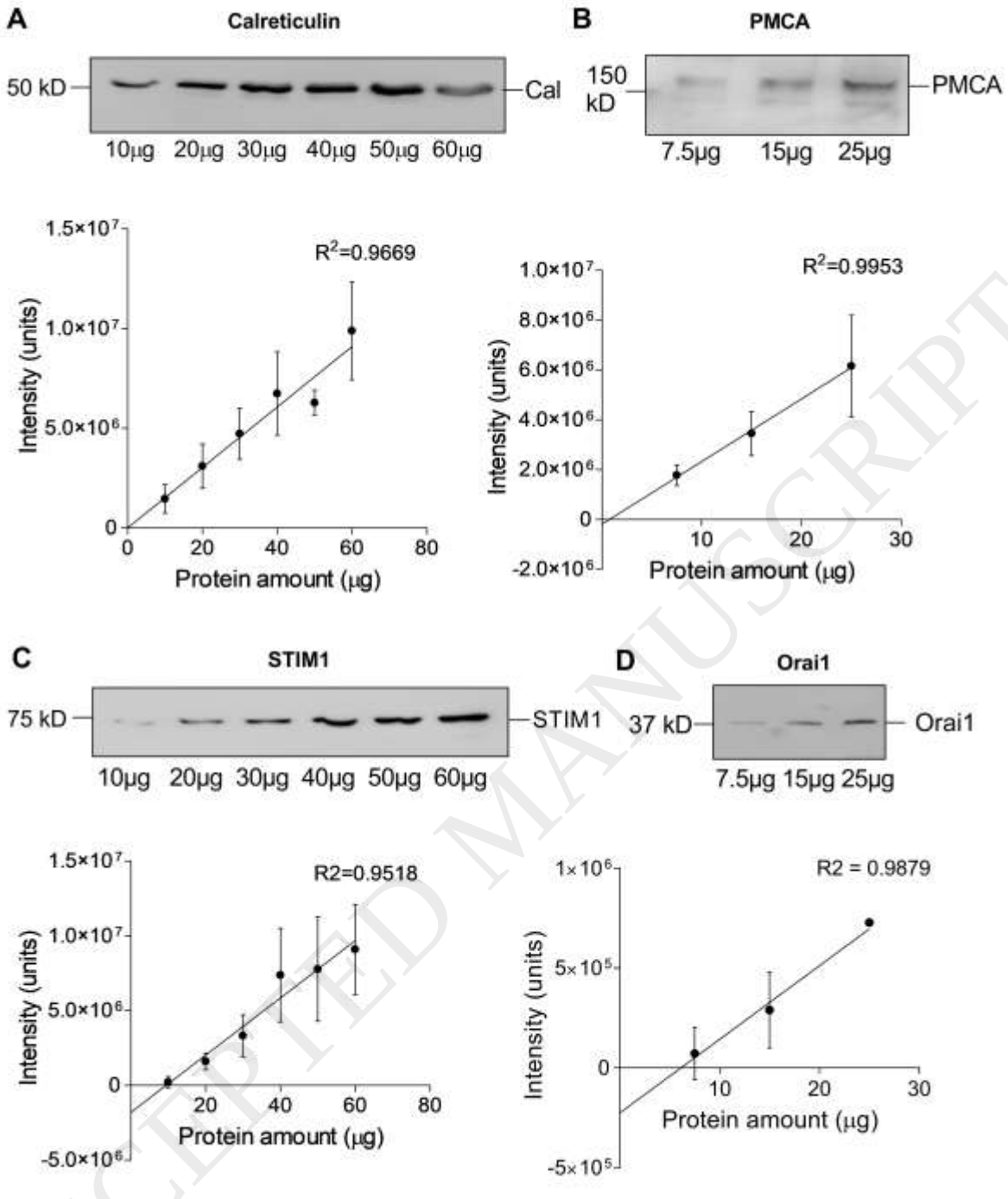

Figure 1.

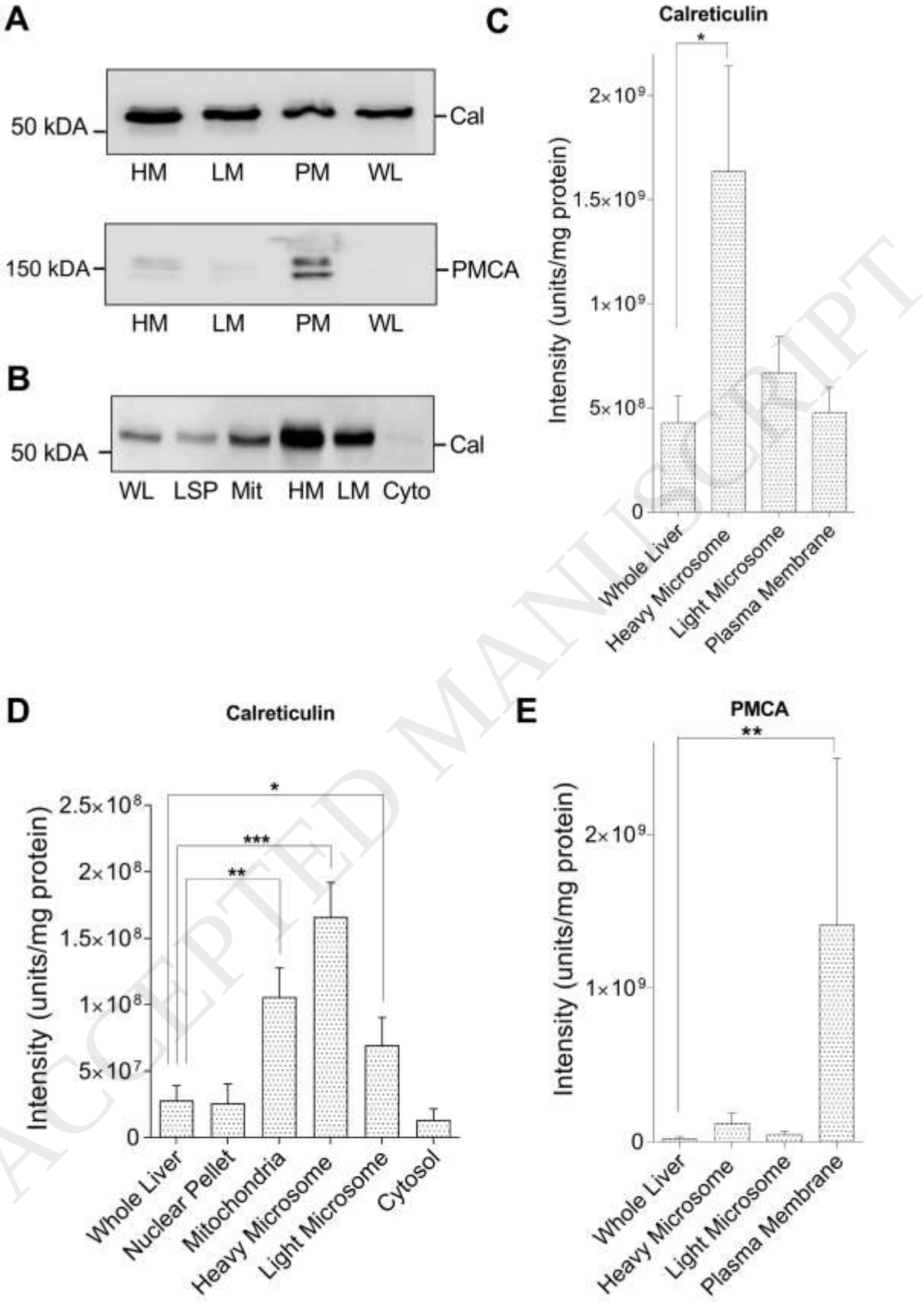

Figure 2.

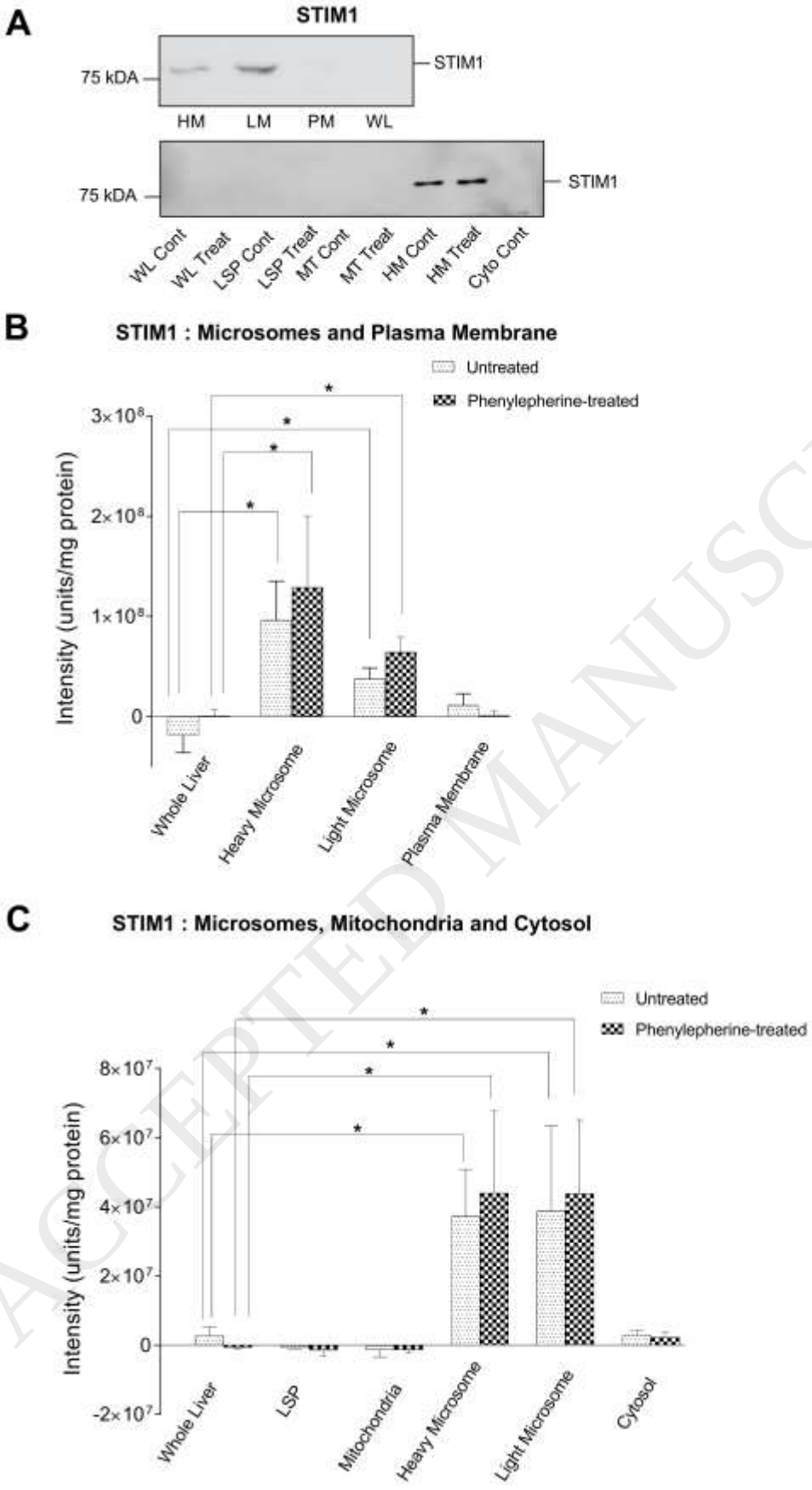

Figure 3.

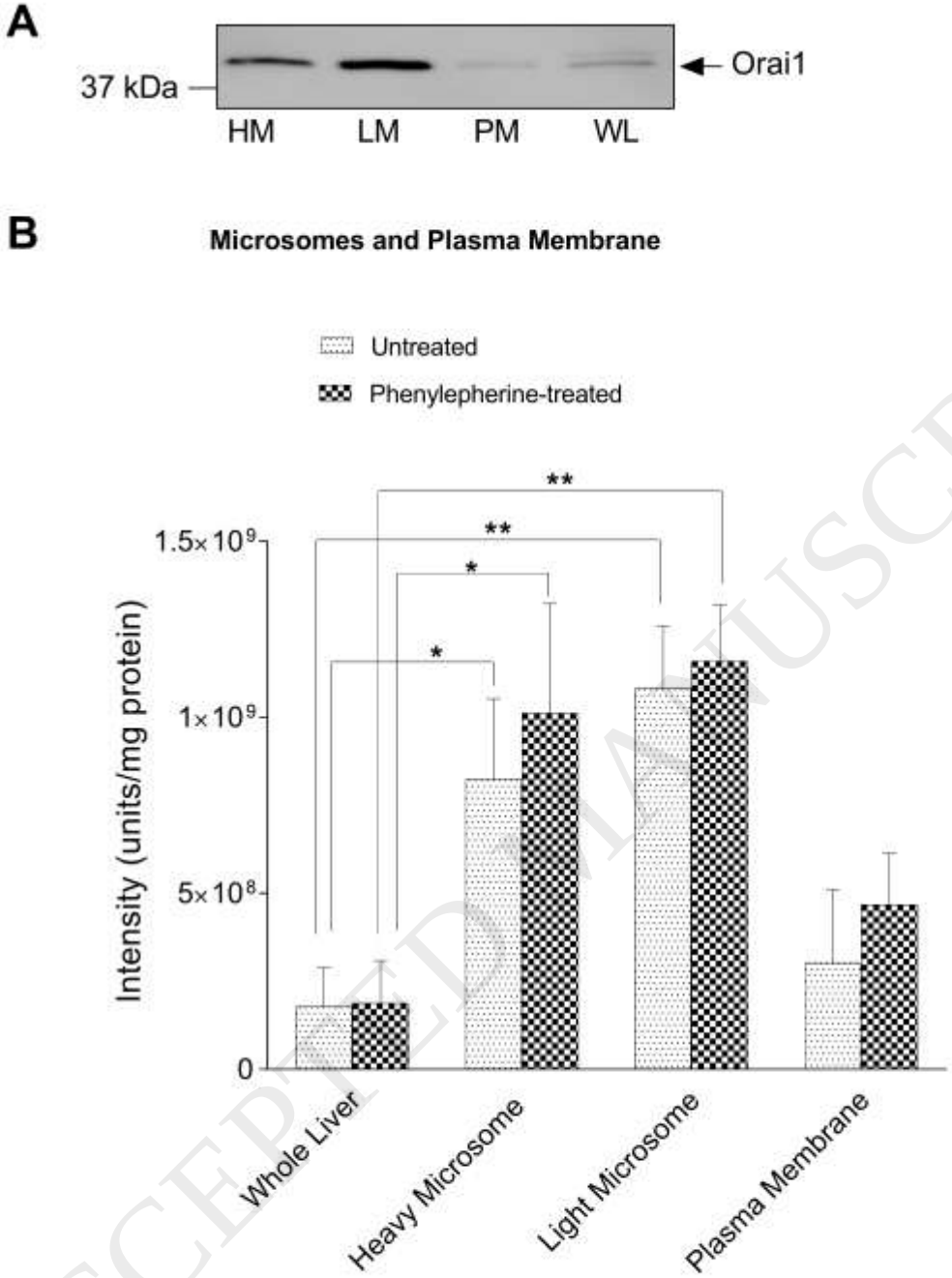

Figure 4.

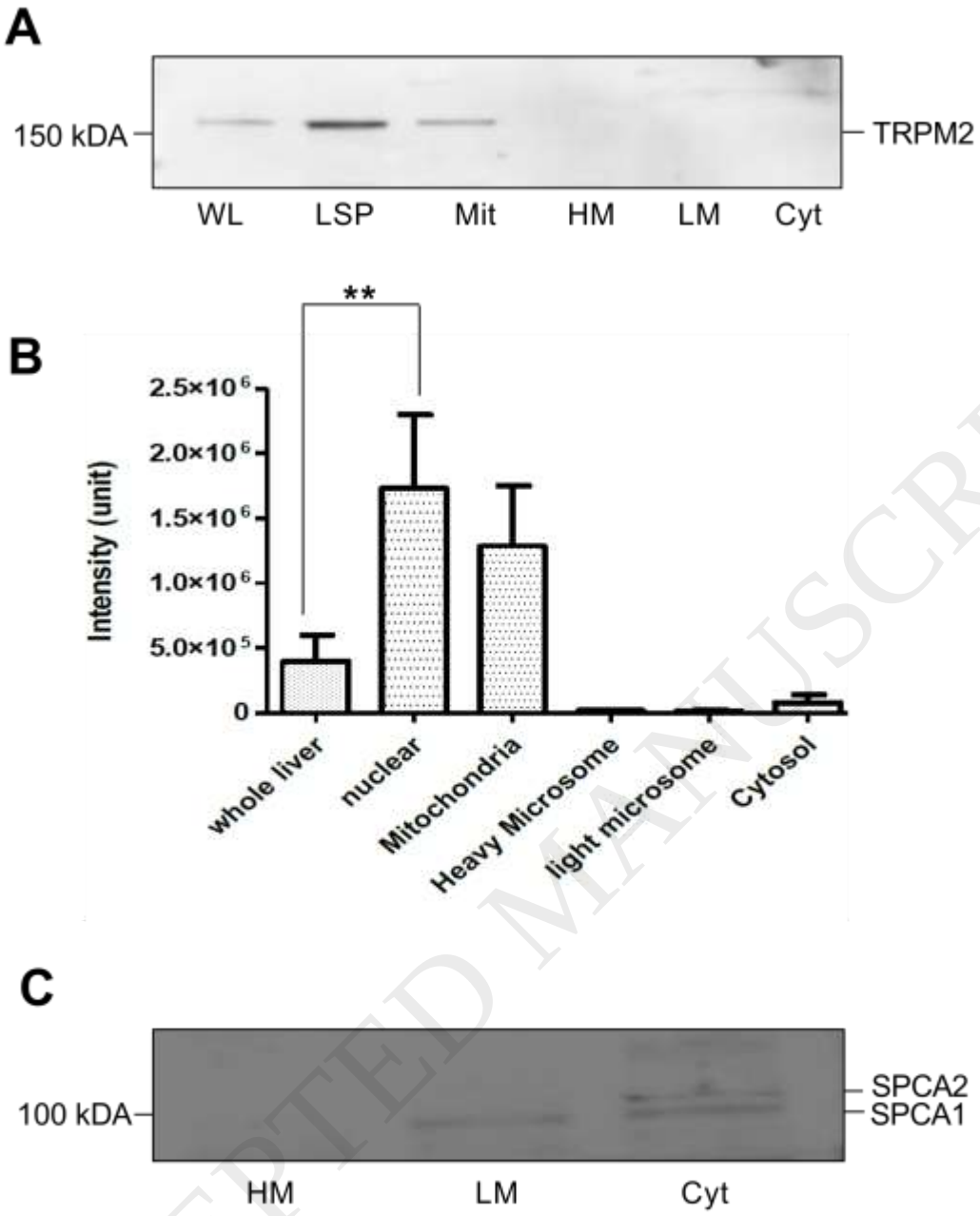

Figure 5.

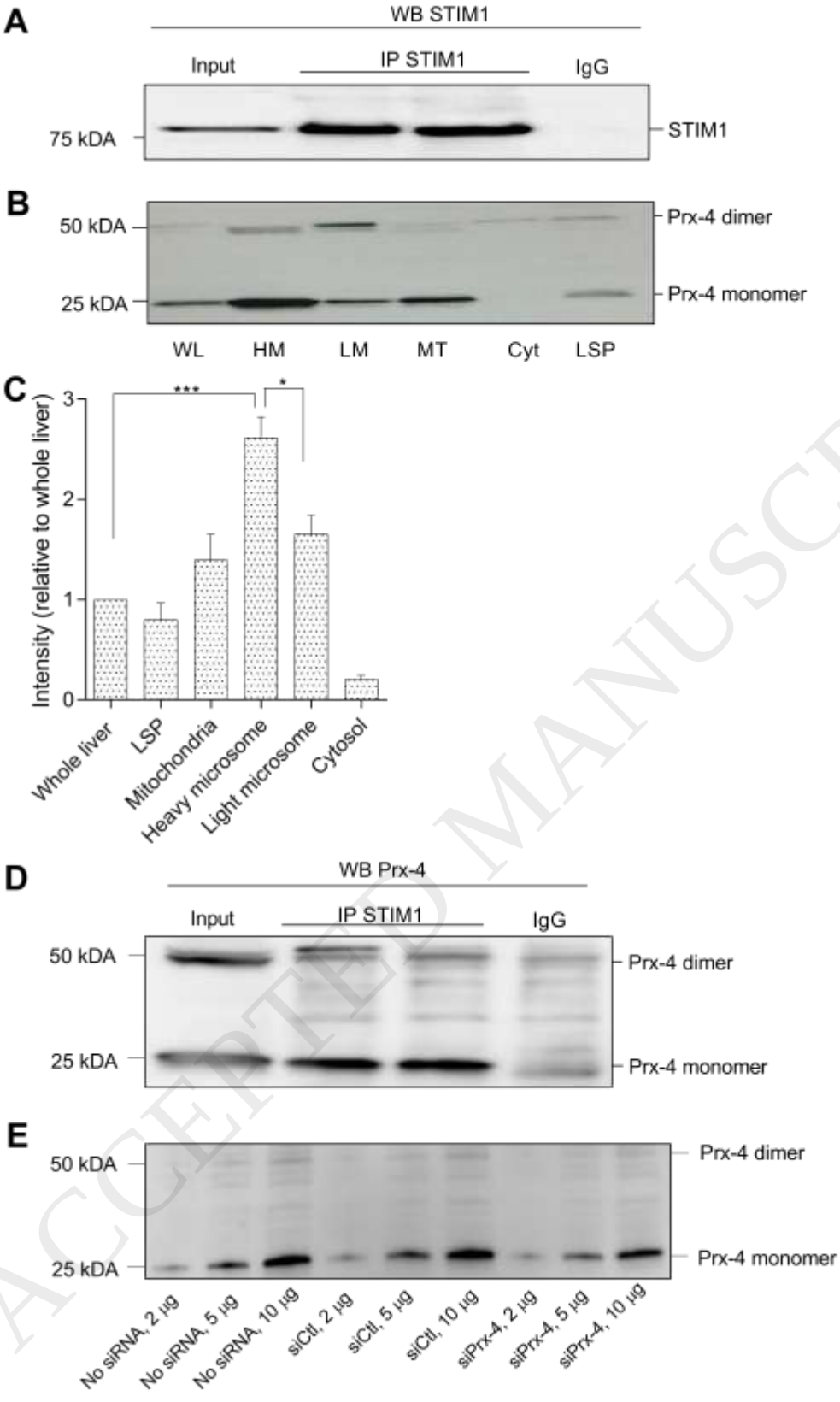

Figure 6.

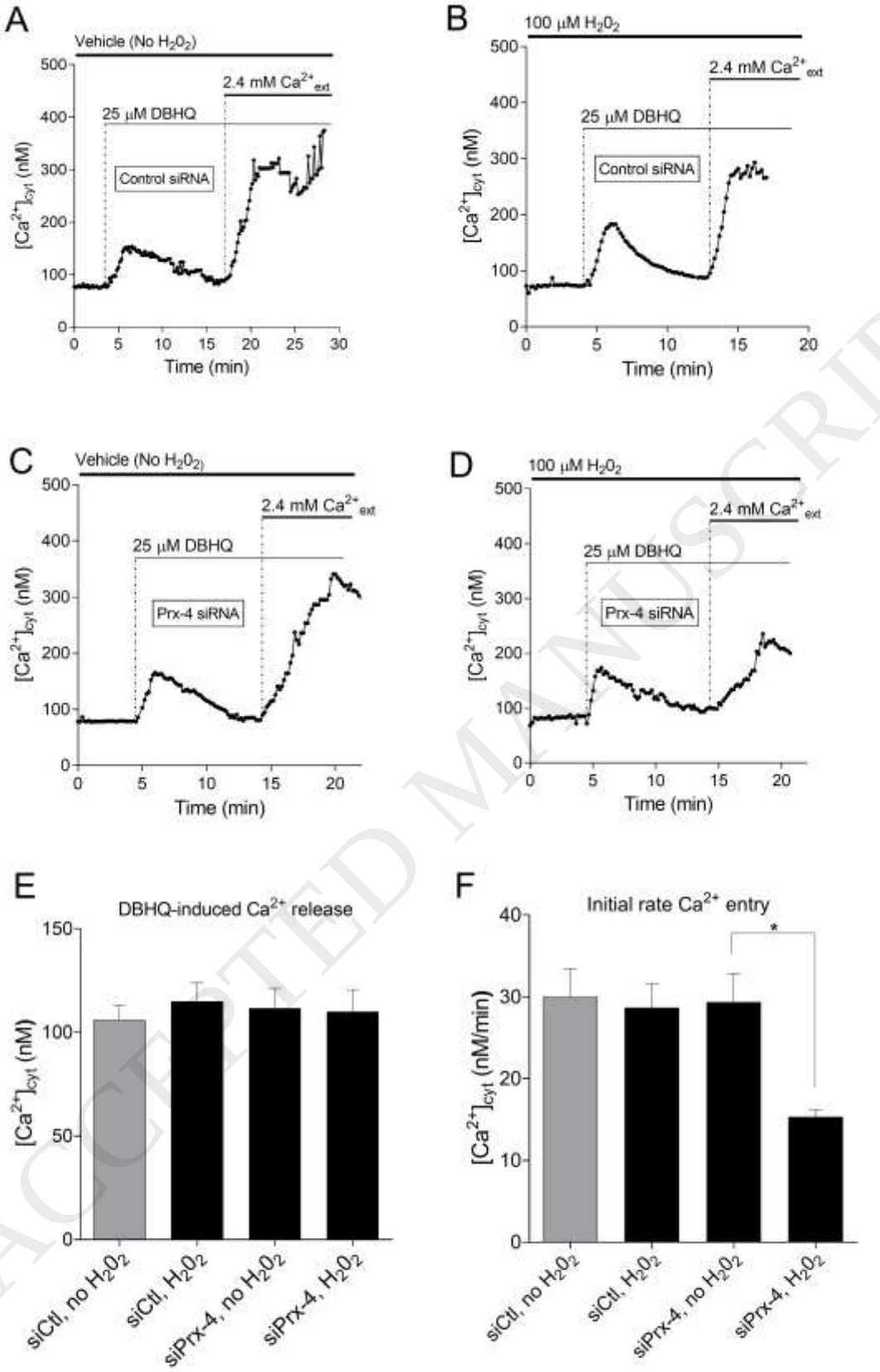

Figure 7.

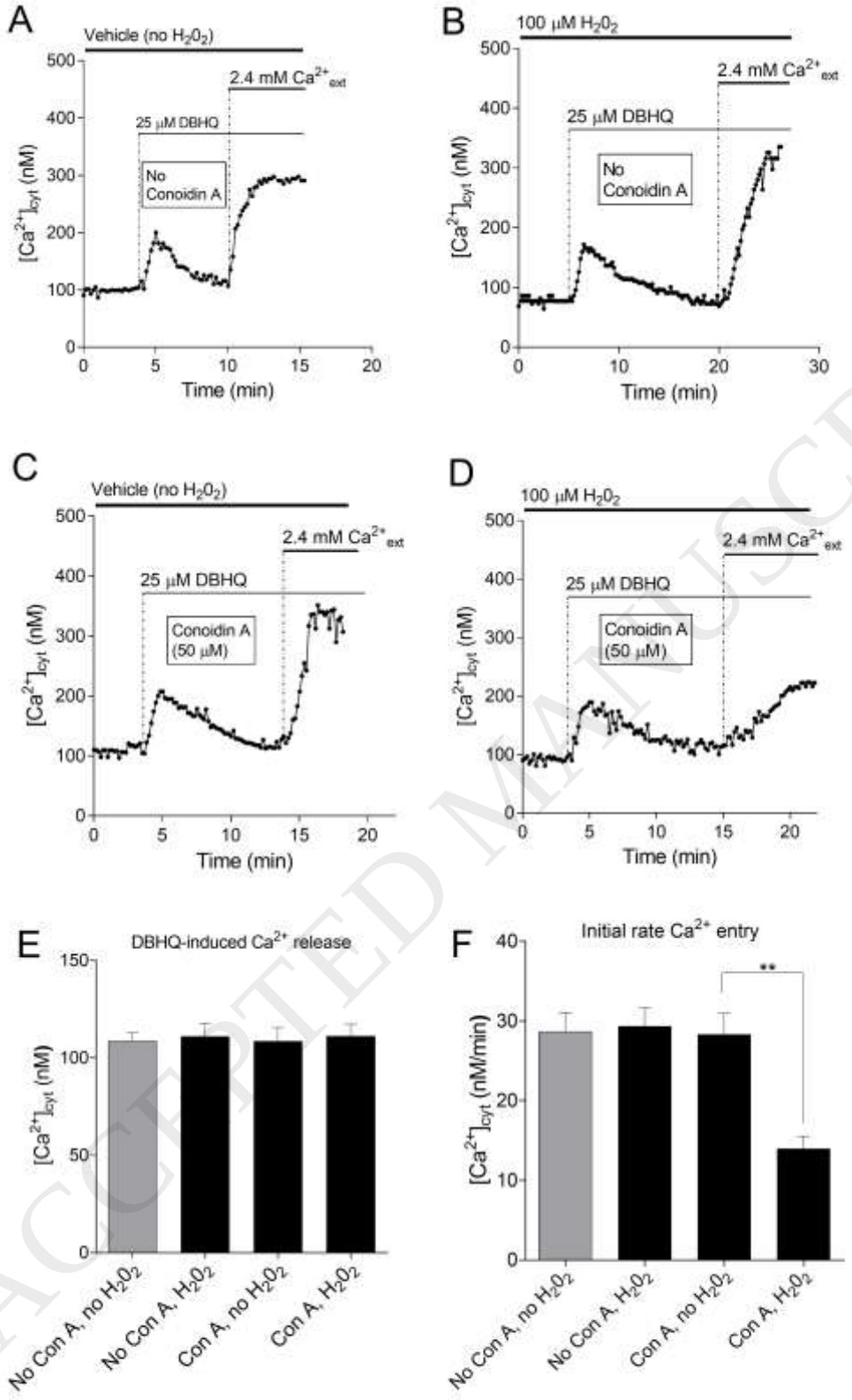

Figure 8.

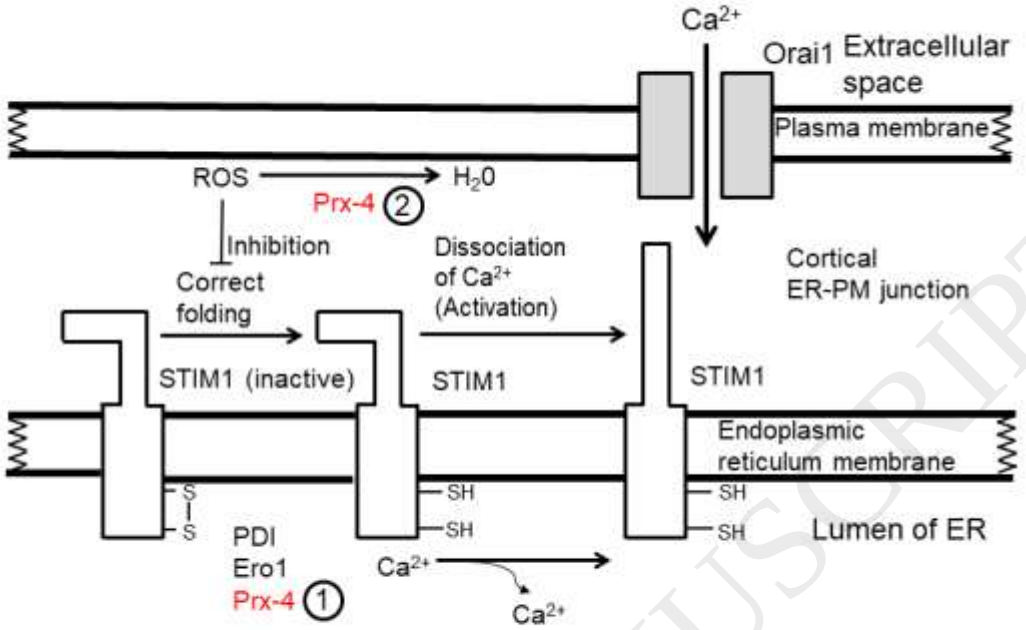

Figure 9

TABLES

Table 1.

Primary and secondary antibodies employed in this study.

Primary Antibody	Source of primary antibody	Dilution of primary antibody	Secondary antibody and dilution	Protein bands detected (estimated size of the band)	Reference to expected size of protein
Anti-calreticulin Goat polyclonal	Santa Cruz Biotechnology, sc-7431 Dallas, Texas, USA	1:2500	Donkey anti goat-HRP 1:5000	50 kDa (Fig. 1A, 2A, Supplemental Data Figs.S1 and S2.)	[36]
Anti-PMCA Mouse monoclonal	Affinity Bioreagent, #MA3-914 Goldern, Colorado, USA	1:2000	Donkey anti mouse-HRP 1:5000	160 kDa (major band) 140 kDa (weak band) (Fig. 1B, 2A, Supplemental Data Figs.S1 and S2.) The 160 kDa band was used for quantitation	[37-39]

Anti-STIM1 Mouse monoclonal	Abcam, # 52458 Cambridge, UK	1:2000	Donkey anti mouse-HRP 1:5000	75 kDa (Fig. 3A, Supplemental Data Figs.S3.)	[69]
Anti- Orai1 Rabbit polyclonal	Alomone Labs, #ACC062 Jerusalem, Israel	1:500	Donkey anti rabbit-HRP 1:5000	45 kDa (glycosylated Orai1) Fig. 4A, Supplemental Data Figs.S4)	[16, 41]
Anti-peroxiredoxin-4 Rabbit polyclonal	Biosensis, # R-1593-100 Thebarton, South Australia	1:1000	Donkey anti rabbit-HRP 1:5000	25 kDa (monomer) and 50 kDa (dimer) (Fig. 6B) The sum of the 25 and 50 kDa bands was used for quantitation	[53, 55]
Anti-TRPM2 Sheep polyclonal	Abcam, #ab63015 Cambridge, UK	1:500	Donkey anti-sheep-HRP 1:5000	150 kDa (Fig. 5A)	[34]
Anti-SPCA 1 and 2 Rabbit polyclonal	Santa Cruz #sc Dallas, Texas, USA -134450	1:350	Donkey Anti Rabbit-HRP 1:2000	100 kDa SPCA 1) 110 kDa SPCA 2) (Fig. 5C)	[76]

Table 2.

Distribution of STIM1 and Orai1 in subcellular fractions derived from untreated and phenylephrine-treated livers.

[a]Results, expressed as band intensity (arbitrary units) per total volume of the given fraction, are the means ± SEM obtained from western blots of subcellular fractions derived from 5-6 (STIM1) and 4 (Orai1) livers.

Subcellular Fraction	Amount of STIM1 in each fraction[a]				Amount of Orai11 in each fraction[a]			
	Untreated liver		Phenylephrine-treated liver		Untreated liver		Phenylephrine-treated liver	
	Arbitrary intensity units per fraction	Percentage of amount in liver homogenate	Arbitrary intensity units per fraction	Percentage of amount in liver homogenate	Arbitrary intensity units per fraction	Percentage of amount in liver homogenate	Arbitrary intensity units per fraction	Percentage of amount in liver homogenate
Liver Homogenate	-3.6±19	100	17±47	100	9.0±2.9	100	83±36	100
Heavy microsomes	39±17	85	50.1±29	76	3.9±0.8	44	39±0.8	45
Light microsomes	5.6±2.0	12.5	16.1±3.2	24	2.4±2.6	27	3.9±0.8	27
Plasma membrane	0.04±0.04	0.09	0.002±0.01	0.003	0.03±0.002	0.03	0.07±0.04	0.09
Sum of subcellular fraction (% of homogenate)		101		100		71		72

Table 3.

Proteins detected by LC/MS in the precipitate resulting from the immunoprecipitation of STIM1 from the heavy microsomal subcellular fraction prepared from untreated livers.

[a] Calculated percentage of the protein sequence determined from the individual unique peptides. [b] Number of unique peptide matches with the protein sequence. [c]The results shown were obtained following the analysis of proteins in the precipitates obtained from the immunoprecipitation of STIM1 from heavy microsomal subcellular fractions prepared from two untreated livers.

Accession No.	Coverage (% AA)[a]	No. of Peptides[b]	Score	Protein Name[c]
P84903	25.55	15	79.86	Stromal interaction molecular 1(STIM1)
D4ABS3	36.96	5	58.74	HistoneH2B
P20762	14.29	4	44.99	Ig gamma-2C chain C region
Q9Z0V5	21.98	5	31.65	Peroxiredoxin-4
Q5BJT0	11.44	4	18.02	Arginine and glutamate protein 1
Q6IFU7	11.06	4	15.47	Keratin, type I cytoskeletal 42
Q6IFU9	9.72	3	13.81	ProteinKrt16
Q6AXS5-2	6.89	2	10.19	Isoform 2 od plasminogen activator inhibitor 1 RNA-binding protein
F1M7H9	7.58	2	9.75	Protein Luc712 (Fragment)
B2RZB7	20.17	2	7.53	Protein Snrpd1
P02600-2	16.00	2	5.91	Isoform MLC3 Myosin light chain 1/3, skeleton muscle isoform
F1LRK8	4.56	2	5.08	Actin-related protein 3
D4A1G4	30.00	2	4.86	Cytochrome b5
B5DES0	16.10	2	4.20	Protein Snrpd2